

VENT SIZING FOR PHENOLIC REACTORS

Fortunato Ritorto

ECOPROGETTI SRL, C. Susa 6, 10098 Rivoli, Italy

E-mail address: aria@ecoprogettisrl.it

May 2025

CONTENTS

ii

ABSTRACT	iv
INTRODUCTION	1
1. <u>PRESENTATION OF THEORETICAL FORMULAS</u>	2
1.1. KINETICS OF EXOTHERMIC REACTIONS	2
1.1.1. <u>Case of a single reaction</u>	2
1.1.2. <u>Presence of several simultaneous reactions</u>	9
1.2. THE REACTION BETWEEN PHENOL AND FORMALDEHYDE	13
1.2.1. <u>Reaction mechanisms</u>	13
1.2.2. <u>Influence of curing on the heat of reaction</u>	18
1.3. EMERGENCY DISCHARGE FLUID DYNAMICS	23
1.3.1. <u>Relief area calculation</u>	23
1.3.2. <u>Two-phase flow calculation</u>	32
1.3.3. <u>Thrust calculation</u>	37
1.3.4. <u>Identifying the flow conditions</u>	39
2. <u>DESCRIPTION OF EXPERIMENTAL TESTS</u>	43
2.1. THE PILOT APPARATUS	43
2.2. PERFORMED TESTS	44
3. <u>GETTING THE THERMOKINETIC PARAMETERS</u>	46
3.1. TESTS WITH THE PILOT REACTOR	46
3.2. MEASUREMENTS ON INDUSTRIAL REACTOR	53
4. <u>RUPTURE DISK SIZING</u>	56
4.1. PRELIMINARY REMARKS	56
4.2. CHOICE OF DISK SET PRESSURE	58
4.3. VENT AREA CALCULATION IN TWO-PHASE FLOW CONDITIONS	60
4.4. ALL VAPOUR EMISSION	66
5. <u>EMISSION CONTAINMENT</u>	69

6. <u>PRECAUTIONS TO AVOID REACTION RUNAWAY</u>	74
APPENDIX I	
CALCULATION OF FLOW REDUCTION COEFFICIENT	77
APPENDIX II	
SAFETY VALVE SIZING	85
APPENDIX III	
MEAN VALUE OF SPECIFIC THERMAL POWER	92
REFERENCES	95

ABSTRACT

First of all a reminder is given of the equations that describe the temperature increase with time of a reacting mass in adiabatic conditions.

A discussion follows on the related plots, obtainable through tests with laboratory adiabatic calorimeters and pilot or industrial reactors, with particular reference to the problem of extrapolating to industrial reactors the results got through small apparatuses, primarily in the case of complex reactions as the phenol-formaldehyde one.

The mechanisms of the two fundamental phases of this reaction (methylolation and condensation) are reminded, trying to correlate the total temperature increase (and therefore the overall heat of reaction) with the energy contributions of the single phases and with the molar ratio (formaldehyde/phenol) characterizing the reacting mixture.

Then we report the calculation procedures suggested by DIERS for sizing emergency relief devices, with reference to the so-called “tempered” systems in which pressure and temperature are reciprocally correlated by the law of variation of the vapour pressure of the solvent (that is water in our case).

For relief area evaluation we used the equation suggested by Leung supposing a two-phase homogeneous discharge flow (HEM). For determining the specific flow, including the reduction effect due to the pipe downstream the relief device, we used the “ ω method” by the same Author.

For the calculation of the reduction coefficient, which corrects the expression of flow through an ideal nozzle, we worked out some approximate simplified formulas, which apply to the most customary discharge configurations.

An account follows of performed tests and used apparatuses, with the consequent working out of the results to obtain the thermokinetic constants (ΔH , E, K) characterizing the reaction of phenolic resins formation with basic catalysis.

In particular we evaluated the influence of a variation of catalyst concentration around the values of normal use.

At last we worked out a complete and detailed numerical example, studying the influence on the relief area both of rupture disk set pressure and reactor maximum allowable pressure, and of the possible inaccuracy which affects one of the thermokinetic parameters (ΔH).

The example includes the evaluation of the thrust exerted on the discharge pipe and the preliminary sizing of the most suitable containment system for the emission.

A mention is also made of the useful precautions to prevent or contain the quick temperature rise and so to avoid the rupture disk intervention.

Keywords: Phenol–formaldehyde runaway reaction; Emergency pressure relief; ω method; Rupture disk sizing; Emergency emission containment and prevention

INTRODUCTION

Recurrence of devastating explosions of phenolic reactors, even in recent times, led some Italian companies in the sector of decorative laminates to review the design methods both of the relief area of rupture disks, widely used to face emergency situations in phenol-formaldehyde runaway reaction, and of containment systems for the consequent emissions.

Generally the point of reference for chemical reactors emergency relief devices is set by the results got by DIERS (Design Institute for Emergency Relief Systems), within the intense program of studies and trials carried on in the United States in the first half of the eighties and sponsored by the main chemical companies of the world.

Those results gave origin besides to design methods collected in a proper project manual [14].

For the specific system under examination (base-catalyzed phenol-formaldehyde reaction) a preliminary research pointed out the great lack of specific data in literature and the inconsistency of the few found out.

Owing to the difficulty, better specified in the following, in getting meaningful data through the existing Italian laboratories, we decided to support the necessary theoretical formulations with experimental data obtained both through the direct operation of industrial reactors and through a small pilot plant, employing the exact production recipes and able to simulate as accurately as possible the behaviour of full scale reactors.

In the following we will first illustrate the theoretical principles which are the basis of the formulas used to draw the path, normal or uncontrolled, of an exothermic reaction; then we will describe the experimental tests and the way through which we got from them the fundamental parameters to put into the theoretical formulas; at last we will go through a detailed sizing example.

1. PRESENTATION OF THEORETICAL FORMULAS

1.1. KINETICS OF EXOTHERMIC REACTIONS

1.1.1. Case of a single reaction

We will suppose that the course of reaction with time (t) can be correlated with the concentration (x) of only one of the reagents, according to the expression:

$$\frac{dx}{dt} = -Kx^n \quad (1.1)$$

where n is the order of reaction and K is the rate constant.

This one, on the basis of Arrhenius expression, is equal to:

$$K = K_r \cdot \exp\left[\frac{E}{R}\left(\frac{1}{T_r} - \frac{1}{T}\right)\right] \quad (1.2)$$

where K_r is the value of K at a reference temperature T_r , T ($^{\circ}\text{K}$) is the absolute temperature of the reacting mass, E is the activation energy (kcal/kmole) and R is the universal gas constant (1.987 kcal/kmole/ $^{\circ}\text{K}$).

If ΔH (kcal/kmole) is the heat of reaction, generated by one kmole of the considered reagent, the following thermal balance will hold, according to which this heat partly goes to increase the temperature of the reacting mass M (kg) and of reactor walls, partly is transmitted to the cooling liquid (when used) through coils, jacket or reflux condenser.

$$-\Delta H \cdot dx \cdot V_l = MC_p \phi \cdot dT + US(T - T_c) \cdot dt \quad (1.3)$$

In the previous expression ΔH has been considered positive in case of exothermic reaction, V_l is the volume of the reacting mass (having specific heat C_p), U is the overall heat transfer coefficient between mass and cooling liquid (having temperature T_c), S is the heat transfer area, ϕ is a coefficient that takes into account the thermal capacity of reactor walls and agitator, which are supposed in every moment at the same temperature T of the contents.

It is given by:

$$\phi = 1 + \frac{M_r C_{p,r}}{MC_p} \quad (1.4)$$

where M_r and $C_{p,r}$ are the mass and the specific heat of the metal parts.

In case of loss of reaction control the last term of (1.3) can normally be disregarded (heat transfer becomes negligible, for instance owing to lack of cooling liquid or of suitable mass agitation): reaction goes on in adiabatic conditions.

In this case by direct integration of (1.3) we get:

$$x_0 - x = \frac{M \cdot C_p \cdot \phi}{V_l \cdot \Delta H} (T - T_0) \quad (1.5)$$

where x_0 and T_0 are the start values (for $t = 0$).

For $x = 0$ (no more reagent) we have

$$T = T_f = T_0 + \Delta T_{ad} \quad \text{with} \quad \Delta T_{ad} = \frac{V_l \cdot \Delta H \cdot x_0}{M \cdot C_p \cdot \phi} \quad (1.6)$$

where ΔT_{ad} turns out to be the temperature increase of the reacting mass, in adiabatic conditions, as a result of the total consumption of the reference reagent.

From (1.5) and (1.6) we get:

$$\frac{x}{x_0} = \frac{T_f - T}{T_f - T_0} = \frac{T_f - T}{\Delta T_{ad}} \quad (1.7)$$

Differentiating (1.7) and substituting in (1.1) we get

$$-\frac{dx}{dt} = \frac{x_0}{\Delta T_{ad}} \frac{dT}{dt} = Kx^n = Kx_0^n \left(\frac{x}{x_0}\right)^n = Kx_0^n \left(\frac{T_f - T}{\Delta T_{ad}}\right)^n = K \left(\frac{x_0}{\Delta T_{ad}}\right)^n (T_f - T)^n$$

from which

$$\frac{dT}{dt} = K \left(\frac{x_0}{\Delta T_{ad}}\right)^{n-1} (T_f - T)^n \quad (1.8)$$

Time t necessary to reach a pre-established temperature T is given by

$$t = \frac{\left(\frac{\Delta T_{ad}}{x_0}\right)^{n-1}}{K_r} \cdot \int_{T_0}^T \frac{e^{\frac{E}{R}\left(\frac{1}{T} - \frac{1}{T_r}\right)}}{(T_f - T)^n} dT \quad (1.9)$$

This integral can be solved only numerically (for instance with Cavalieri-Simpson method).

The plot of temperature against time, which may be obtained from the previous expression or experimentally, is the one of fig. 1 (for three values of ϕ , other conditions being equal).

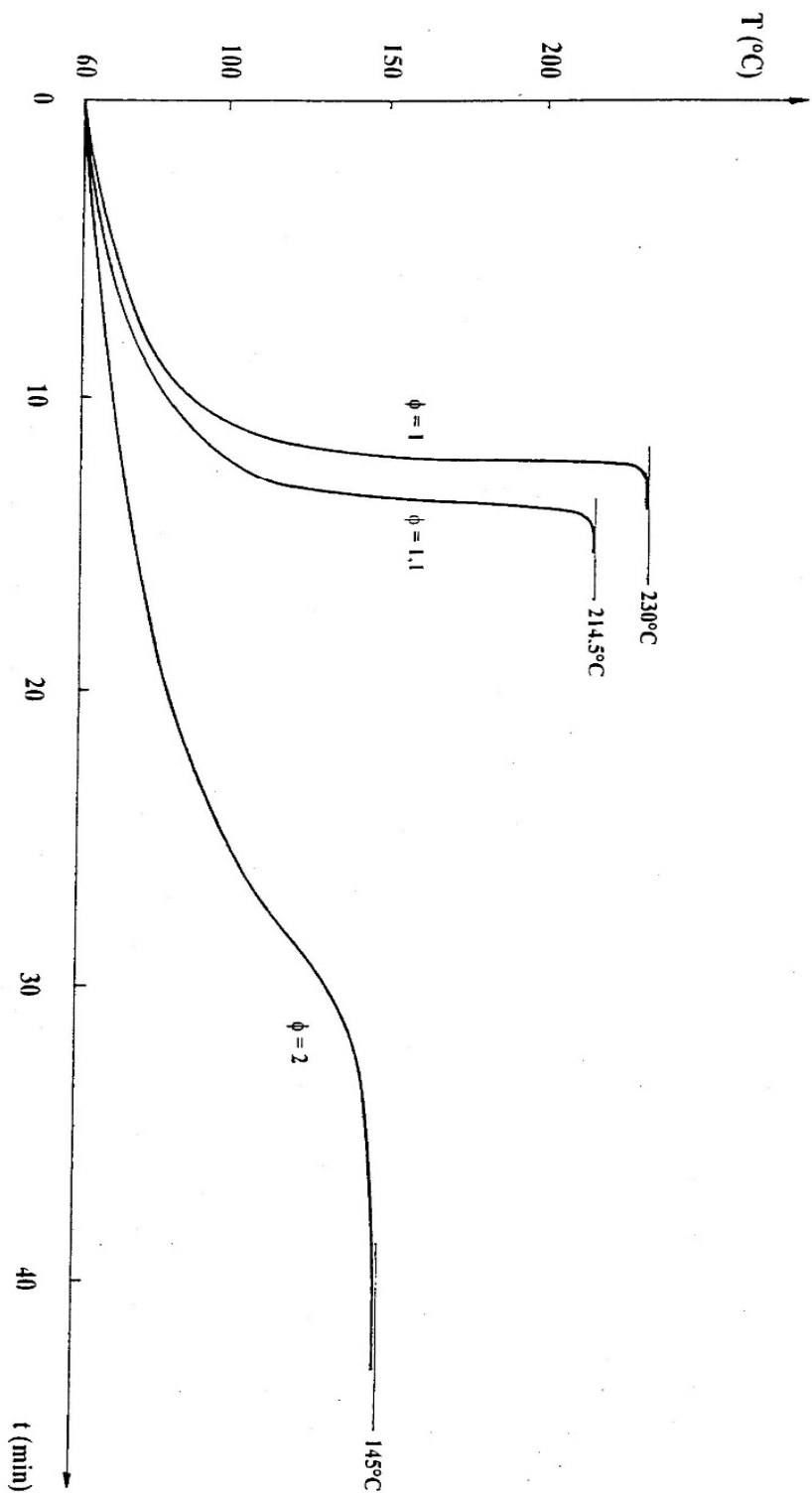


Fig. 1 – Adiabatic temperature rise for various ϕ values

It is easily explained, taking into account that at low temperatures reaction is slow, because K , given by (1.2), is small: little heat is generated and therefore temperature grows slowly.

However, when T increases, the rate constant K begins to rise exponentially, together with reaction rate, generated heat and therefore mass temperature, with a consequent self-exalting of the phenomenon. At a certain point the reagent concentration, in progressive depletion, drops so much as to offset the effect of temperature on K , until, in a rather sharp way, both x and reaction rate fall to zero, and temperature stops rising. It is interesting to remark that the lower ϕ is, the quicker the temperature rises, as also the analysis of expression (1.8) shows. This is however a matter of course, because almost all generated heat goes to warm up the reacting mass, without being dissipated into the walls.

To size relief areas in emergency situations we need, as it is easy to guess and as we will see in detail, the values of dT/dt in the temperature range (or in the pressure range) in which there is the intervention of the suitable devices (normally rupture disks).

The reason is that dT/dt is directly proportional to the thermal power Q generated in every moment by the reaction (in adiabatic conditions $Q = MC_p \phi \cdot dT/dt$).

If we had at our disposal the experimental plot of fig. 1, obtained through a test apparatus having a ϕ close to the one of the industrial reactor, it would be sufficient to take dT/dt from such a plot in correspondence with the temperatures of interest, without the need of knowing anything about reaction thermodynamics and kinetics.

An industrial reactor has a ϕ of about 1.04÷1.05. A conservative value ($\phi = 1$) is however normally assumed.

Laboratory or pilot apparatuses have variable ϕ according to the model: they go from $\phi = 1.05$ of VSP (Vent Sizing Package, set up within DIERS studies) and of the similar PHI-TEC (later introduced) to 1.5÷3 of ARC (Accelerating Rate Calorimeter, available since the late seventies).

Particularly if ϕ is noticeably greater than 1, it is necessary to use the above expressions to obtain mathematically the actual curve of dT/dt for $\phi = 1$, starting from the experimental plot (valid for the ϕ value typical of the apparatus).

If ϕ is slightly greater than 1, corrections turn out to be modest, but they rise very speedily when ϕ grows, particularly if the temperature of interest is much higher than T_0 . In the ARC case the correcting factors easily reach dozens of times, as it can be shown mathematically (*) and as it appears clearly from fig. 1 and fig. 2 (see the following paragraph).

Let us see then how we can get from expression (1.8), having an experimental plot like the one of fig. 1, the various thermodynamic and kinetic parameters (ΔH , E , n , K_r), to proceed eventually to the reconstruction of the curve of temperature against time, valid for $\phi = 1$.

First of all from the experimental plot we can generally read directly T_0 and $T_{f,\phi}$ (which is the value of T_f coming out from the use of an apparatus having a certain $\phi > 1$).

We have, for (1.6):

$$\Delta T_{ad,\phi} = T_{f,\phi} - T_0 \quad \text{and} \quad \Delta H = \frac{MC_p\phi}{V_l x_0} \cdot \Delta T_{ad,\phi}$$

We must then evaluate from the plot of T against t the tangent dT/dt for various T values (most laboratory apparatuses give directly the curve of dT/dt against T).

We calculate $y = \ln \left[\frac{dT}{dt} / (T_{f,\phi} - T)^n \right]$ for some n values (for instance $n = 1$, $n = 1.5$, $n = 2$).

Then we draw the curve of y against $1/T$.

(*) If $n = 0$, dT/dt is proportional to ϕ for every value of T .

If $n \neq 0$, dT/dt is proportional to ϕ only for T very close to T_0 . To get for instance the ratio between the maximum values of dT/dt (for $\phi = 1$ and for a generic ϕ), it is sufficient to take into account that they come out for

$$T = T_M = \frac{E}{2nR} \cdot \left(\sqrt{1 + 4T_f nR/E} - 1 \right)$$

and to calculate the two values of dT/dt for $T = T_M$ through (1.8). Notice that ΔT_{ad} , T_f and therefore T_M depend on ϕ .

As from (1.8) y turns out to be equal to $\ln K$ (apart from a constant) and as $\ln K$, owing to expression (1.2), is a linear function of $1/T$, we get a straight line if the hypothesis of a single reaction (or pseudo-reaction, in the sense better specified in the following) with a simple n -order kinetics was correct.

In particular we are able to determine the order n of reaction kinetics on the basis of which of the drawn curves (for various n values) best fits a straight line.

The slope of that line is equal to $-E/R$ and gives therefore the activation energy.^(*)

The value of K_r can be obtained for instance from the ordinate y_r of the interpolating line for $1/T = 1/T_r$ (taking obviously into account the constant which differentiates y from $\ln K$).

$$\text{We obtain } K_r = e^{y_r} \left(\frac{\Delta T_{ad,\phi}}{x_0} \right)^{n-1}$$

At this point we can get the values of dT/dt , necessary for sizing the rupture disk, from (2.8) applied to the case of $\phi = 1$, that is using for ΔT_{ad} the value

$$\Delta T_{ad,1} = \frac{\Delta H \cdot V_l \cdot x_0}{M \cdot C_p} \quad \text{and for } T_f \text{ the value } T_{f,1} = T_0 + \Delta T_{ad,1}$$

T_0 may be now different from the value of the experimental test; the new value will be the one fixed within the assumed failure scenario.

If that scenario foresees the same x_0 value as in the laboratory test, to calculate $\Delta T_{ad,1}$ we can use the expression $\Delta T_{ad,1} = \phi \cdot \Delta T_{ad,\phi}$, where ϕ and $\Delta T_{ad,\phi}$ are the values related to the experimental apparatus.

We should like eventually to remark that the values of dT/dt are very sensitive to small changes in the parameters that determine them (ΔH , E , K_r , n).

(*) It is customary to evaluate E/R on the basis of the slope for $T = T_0$ of the curve $\ln dT/dt$ against $1/T$. Actually from (1.8) we get

$$\left(\frac{d \left(\ln \frac{dT}{dt} \right)}{d \frac{1}{T}} \right)_{T=T_0} = -\frac{E}{R} + n \frac{T_0^2}{\Delta T_{ad}}$$

Neglecting the second addendum may involve an error of about 10%.

If those parameters were got independently between them, for instance from various literature sources or from experiments of different nature, it would be easy to attain very heterogeneous results just depending on the selected sources. And no wonder, considering for instance that, in the case of phenolic resins production:

- literature data are often in poor agreement between them,
- they usually refer to the single reactions of addition of formaldehyde to phenol or of condensation of several aromatic rings between them, while the quick adiabatic temperature rise, typical of emergency situations, corresponds to an overall pseudo-reaction which is a mixture of the two.

The method here proposed “forces” the combination of values used for the various parameters to faithfully describe the wide experimentally determined part of the curve $T = T(t)$, which, apart from small corrections, is the one that gives then directly the required results (that is the values of dT/dt). Such small corrections and extrapolations, carried out through theory, are reliable just because they are of modest extent and are based on parameters submitted to the cogent aforesaid validation.

1.1.2. Presence of several simultaneous reactions

One of the problems that may occur in practice is that the curve $T = T(t)$ does not correspond to the one theoretically foreseen by (1.9) and (1.8). This may be due to the fact that sometimes there is not an elementary reaction, describable through the expressions (1.1), (1.2) and (1.3), but for instance several consecutive or parallel reactions, which must be simulated with a more elaborate thermodynamic-kinetic model.

The difference between the two cases is pointed out, more than by the curve $T = T(t)$ of fig. 1, by the plot of the logarithm of dT/dt against $1/T$, which, in case of validity of the expression (1.1), has the shape of fig. 2 (reproduced for three values of ϕ), while in presence of two distinct reaction mechanisms it may appear as in fig. 3 (the two “humps” roughly correspond to the two simultaneous reactions, each favoured in itself in a different temperature range).

In this last case, if ϕ of the test apparatus is close to 1 we can use directly the experimental plot to get the values of dT/dt of interest; if on the contrary (as in the ARC case) correction is mandatory, it is inconceivable to apply to such a “humped” curve the previously obtained expressions, only valid for a regular shape as in fig. 2.

The test results turn out to be therefore completely useless, because they cannot be extrapolated.

It may happen in practice that, even in presence of two distinct reaction mechanisms (for instance the addition of formaldehyde to phenol and the condensation of several aromatic rings between them), the overall reaction gives experimentally a regular curve, such as the ones of fig. 2, interpretable as due to a single pseudo-reaction of simple kind, that is described with sufficient approximation by the expressions (1.1), (1.2) and (1.3). In this case the parameters that can be obtained, as already seen, from the experimental plot (ΔH , n , E , K_r) have not a well defined physical-chemical meaning, because they cannot be associated with a specific single reaction mechanism.

They have a pure practical utility, because they allow the extrapolation of results to lower ϕ values.

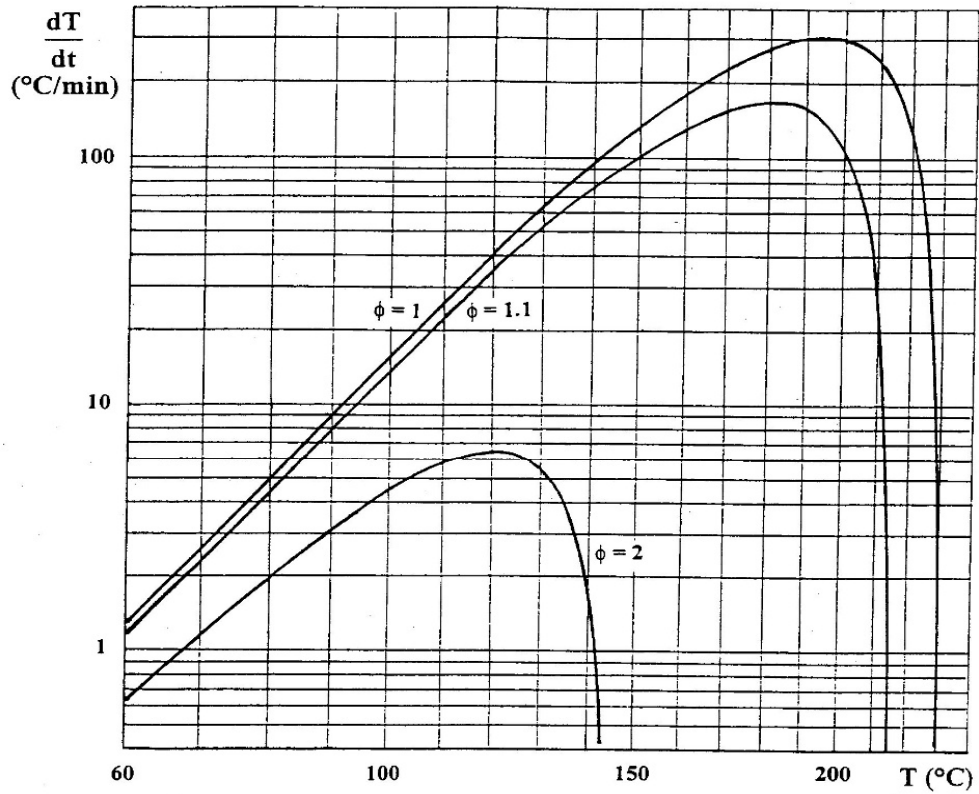


Fig. 2 – Self-heating rate versus temperature for various ϕ values

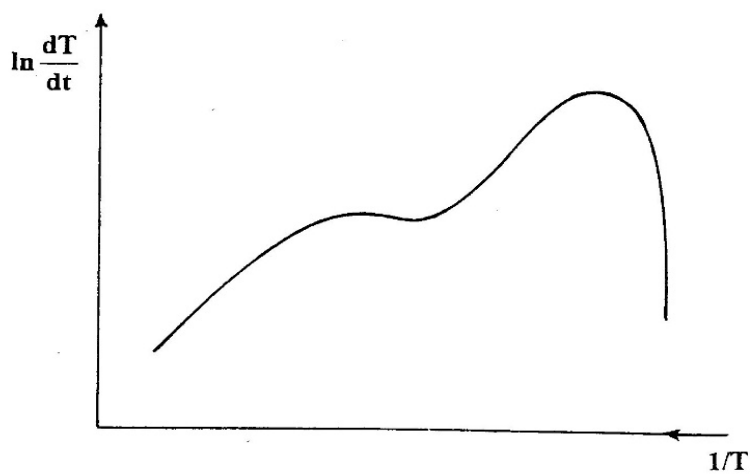


Fig. 3 – Case of two simultaneous reactions

As we already said commenting upon fig. 1, the lower ϕ is, the quicker the temperature rises.

If the rise is sufficiently fast, that is if ϕ is close enough to 1, it is possible that the two concomitant reactions merge into a single apparent overall reaction, without any more the intermediate “trough” of fig. 3.

The reason is not of prompt evidence, but qualitatively it is due to the fact that, if the initial rise, essentially due to the most favoured reaction at low temperatures, is fast enough (because little heat is wasted to warm up the vessel), then it is possible to reach the temperatures, at which also the second reaction is triggered, before the progressive depletion of the reagent that determines the first reaction becomes such as to justify a temporary inflexion of the temperature.

It is clear that also a T_0 value not too low favours a “merging” between the two reactions, for the same reason just explained.

In practice it may happen (and it is what actually happens in the case of base-catalyzed phenolic resins) that if the test apparatus has a ϕ close to 1 an experimental plot without humps is obtained, which allows an easy theoretic correction to go back to the case of $\phi = 1$ (a correction that is however slight, almost superfluous). If the apparatus has a high ϕ (as in the ARC case) a plot with two humps is got, which does not allow an extrapolation of simple type [1, 2]. And this happens just when the correction turns out to be indispensable and very delicate, owing to the size of the multipliers to be applied to dT/dt .

For contingent reasons in Italy (at least up to the beginning of the new century) it was possible to perform tests with ARC, but not with VSP or PHI-TEC, which had no success in our country.

Because of this dead end, to get meaningful data in the case of phenolic resins we thought (at the end of the nineties) to make a small pilot reactor having a ϕ close to 1 (1.1 exactly), able to record the curve of temperature against time up to about 100°C (for reasons of safety and structural simplicity the apparatus could not go to pressures higher than atmospheric).

As the temperatures of interest for rupture disks sizing are, as we will see, of about 110÷130°C, the necessary extrapolation through theoretic formulas (to go back to $\phi = 1$

and to these temperatures higher than 100°C) is not particularly bold, taking into account that several plots obtained with VSP and published [1, 2, 3] (even if referring to different recipes and therefore not directly usable) show that the curve of dT/dt against $1/T$ is regular in all the temperature range of practical interest, without anomalous and sudden rises due to the contingent appearance of new mechanisms.

While we postpone to a following paragraph the description of the apparatus and of performed tests, we remark that the essential features of the small reactor had to be a wall thickness as little as possible (to keep ϕ close to 1) and a good thermal insulation (to simulate adiabatic conditions effectively).

In fact it is clear that a vessel of a few litres has a capability of dissipating heat, compared with the power that can be generated by the contained mass, enormously higher than an industrial reactor (which is virtually adiabatic, towards the surrounding air, even without insulation).

Besides it was necessary, as we will see, to work out a particular method to evaluate ΔH and then ΔT_{ad} and T_f , considering that this last value could not be given directly by the experimental plot (similar to the one of fig. 1), owing to the impossibility of going over 100°C.

1.2. THE REACTION BETWEEN PHENOL AND FORMALDEHYDE

1.2.1. Reaction mechanisms

As already mentioned, the reaction of formation of phenolic resins proceeds in two conceptually distinct stages, which practically tend to overlap: methylation and condensation.

There is first formaldehyde addition to phenol (methylation), with formation of 5 different methylolphenols through 7 possible steps (see fig. 4).

In fact from one to three formaldehyde molecules may react with each phenol molecule, in the two *ortho* and in the *para* positions relative to the hydroxyl group.

Reaction is catalyzed by acids or bases: in this last case, which is the most interesting for us, sodium hydroxide is normally used.

Actually it is the phenate anion, generated by the almost instantaneous reaction between phenol and soda, that acts as the reagent with formaldehyde.

As the molar concentration of phenate is practically identical to the concentration of the charged soda (the molar ratio between catalyst and phenol is equal to a few hundredths), it is natural to expect a rate of the addition reaction approximately proportional to caustic soda concentration, as confirmed by several authors [4].

The values that may be found in literature for the heat of reaction ΔH_M of methylation and for the related activation energy with alkaline catalysis are respectively equal to 4.1÷4.8 kcal/mole (that is for each mole of reacted formaldehyde) and 14÷24 kcal/mole (19÷22 is the range of the most frequent values).

All the 7 possible reactions obey a second order kinetics (rate is proportional to the product of the concentrations of formaldehyde which is present in monomeric form and of phenate or methylolphenate ion at issue).

The evaluation of the curves of concentration against time is extremely complicated, because:

- 1) each of the 7 reactions (some parallel, others consecutive) has its own kinetic constant (normally methylolphenols are more reactive than phenol towards formaldehyde)

- 2) the concentration of the monomeric form of the aldehyde is very different from the total one (it is necessary to subtract the formaldehyde which is present in the form of its oligomers and the amount temporarily fixed by methylolphenols in the form of hemiacetals)
- 3) it is necessary to calculate the concentration of the six anions generated by phenol and methylolphenols according to their respective dissociation constants and to the overall amount of charged soda.

The solution of the onerous resulting system of differential and algebraic equations was numerically calculated through a computer by Zavitsas [5] and checked thanks to the developments of chromatography in those years.

Methylolphenols generated by methylation react between them (and with phenol) to give oligomers which, in a classical resol, are made up by short chains of 2÷5 aromatic rings.

The mechanisms through which such “condensation” happens are essentially the ones of fig. 5.

In alkaline conditions the first reaction, that involves the two methyloic groups, normally proceeds up to compound (2): therefore practically all the aromatic rings of the existing chains are bound by methylene bridges (ether linkages like (1) become stable if condensation is carried on afterwards in neutral conditions).

It is interesting to notice that compound (2), in spite of being the simplest condensation product to mention, actually never occurs, because methylene bridges develop, in resols, between two *para* positions or between a *para* and an *ortho* position, but never between two *ortho* positions.

The ratio between the amounts of the single compounds existing in a resol depends on reaction temperature, catalyst nature and dosage and initial molar ratio between formaldehyde and phenol (which stands between 1 and 3 in the case of resols, while is smaller than 1 for novolaks, obtained with acid catalysis).

Condensation reaction preferably occurs at higher temperatures (70÷100°C) in comparison with methylation. At 60°C the last is definitely prevailing (which explains the two “humps” in ARC plots).

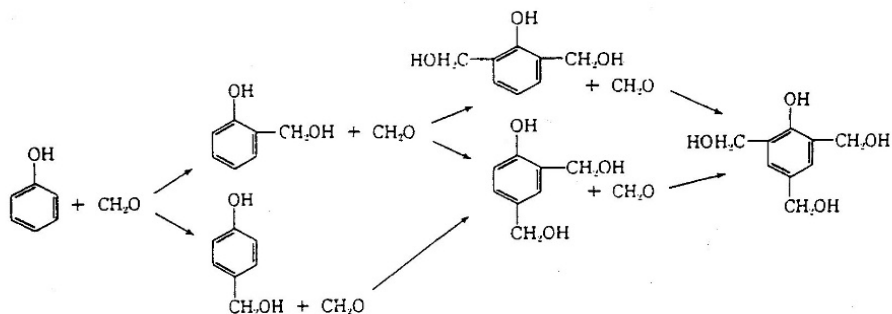


Fig. 4 – Methylation mechanisms

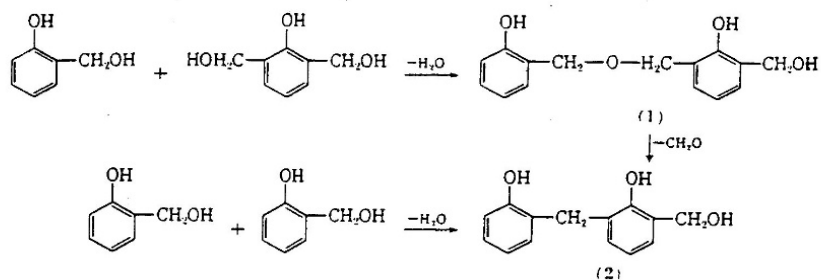


Fig. 5 – Condensation mechanisms

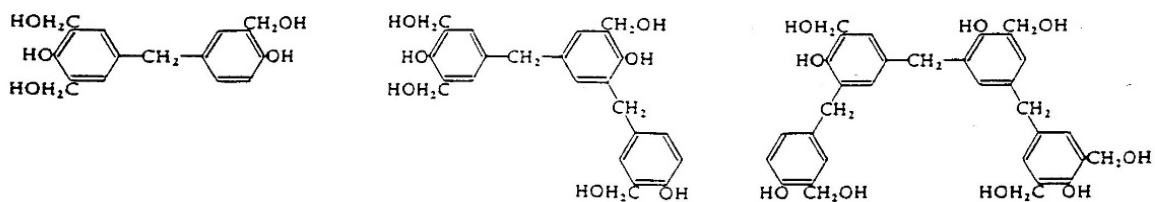


Fig. 6 – Typical compounds in a resol with R = 2

With the formation of a methylene bridge there is the evolution (ΔH_C) of 16.9÷18.7 kcal/mole, with an activation energy of 18.5÷19.3 kcal/mole.

Also condensation is favoured by the presence of acid or basic catalysts.

But while acids act in proportion to their concentration (as they do also in the case of addition), caustic soda has a growing effect up to a molar concentration (much lower than the ones of usual recipes) of a few thousandths of phenol concentration, after which further additions have no more influence on the condensation rate.

With usual catalyst dosages, condensation rate in acid environment is 5÷8 times higher than formaldehyde addition rate, while in alkaline conditions this ratio is equal to about 1/2.

This means that, with acid catalysis, the formation of a molecule of mono-methylolphenol is immediately followed by the condensation of two methylolphenols or of a methylolphenol with a phenol molecule: for each mole of reacted formaldehyde there is then in practice the evolution of $\Delta H_M + \Delta H_C = 21$ kcal (23.5 according to the most conservative evaluations).

In the case of basic catalysis for every condensation act (with evolution of ΔH_C kcal) we have simultaneously about 2 addition acts (with evolution of $\Delta H_M \cdot 2$ kcal): in total for each formaldehyde mole that reacts there is the evolution of $\Delta H_M + \Delta H_C / 2 = 12.6$ kcal (14.2 considering the highest quoted values).

This is only a rough estimate, because the exact ratio between the two reaction rates turns out to be determining (in the case of acid catalysis the knowledge of the exact ratio is clearly much less critical).

This estimate is however confirmed by the value of 10 kcal/mole quoted by Jones [7] and, as we will see, by the data we obtained in our tests.

Another indication may be drawn from the following remark.

Let us consider a resol obtained with a typical molar ratio equal to 2 between formaldehyde and phenol.

It will be on average made up by compounds like the first of fig. 6 (every molecule of which grew up starting from 4 formaldehyde and 2 phenol molecules), or like the second and the third (made up by 6/3 and 8/4 formaldehyde/phenol molecules respectively).

Considering the average values quoted in literature for ΔH_M and ΔH_C , the calories generated by the formation of the three compounds and related to the number of moles of reacted formaldehyde will be respectively equal to:

1) $(4.5 \cdot 4 + 17.8) / 4 = 9.0$ kcal/mole (only one condensation act, 4 addition acts)

2) $(4.5 \cdot 6 + 17.8 \cdot 2) / 6 = 10.4$ kcal/mole

3) $(4.5 \cdot 8 + 17.8 \cdot 3) / 8 = 11.2$ kcal/mole.

More generally, if N is the average number of aromatic rings in resol molecules, R the molar ratio between formaldehyde and phenol, ΔH_R the heat of reaction (per formaldehyde mole) related to resol formation, we easily get:

$$\Delta H_R = \Delta H_M + \frac{\Delta H_C}{R} (1 - 1/N) \quad (1.10)$$

The result, as already seen in the previous example, does not change very much with the number of rings in the chain.

Considering an average value of N ($N = 3$), ΔH_R is worth 10.4 kcal/mole for $R = 2$, while for $R = 1.5$ a slightly higher value is obtained (12.4 kcal/mole).

Also in this method the simplifications are evident (among other things the reasonable hypothesis is done that addition and condensation heats do not depend on the attack positions of formaldehyde and on the kind of reacting methylolphenols), but the obtained order of magnitude is indicative.

We deem however groundless the advice of the British Plastics Federation [8] to conservatively consider equal to 21.5 kcal/mole the overall heat of reaction also in the case of basic catalysis, with the justification that temperature runaway in emergency situations would make condensation uncontrollable in relation to methylolation. Actually temperature increase speeds up both mechanisms, without necessarily and markedly changing the ratio between their respective rates, considering besides that the two activation energies are of the same order of magnitude.

On the other hand our tests, that supply also the value of ΔH_R , have been performed in a temperature range (60-100°C) in which both mechanisms are certainly fully developed.

1.2.2. Influence of curing on heat of reaction

It is suitable to point out that the heat of reaction considered in the previous paragraph, and which we tried to evaluate, is the one corresponding to resol formation. It does not include the heat generated by resin crosslinking process, that begins at temperatures of about 140°C.

In effect neither the normal production process that occurs in phenolic reactors, nor our tests, nor the phase of emergency discharge through rupture disks (if one makes it happen, as we will see, in the correct temperature range) provide for resol crosslinking. Tests with laboratory adiabatic calorimeters, on the contrary, include that phase too, considering that temperature rises in them well over 140°C.

Supposing that the resin reaches the maximum possible crosslinking degree, it is necessary to distinguish the cases with R greater or smaller than 1.5.

In the first case, the moles of formaldehyde exceeding 1.5 times the moles of phenol will find themselves loose at the end of adiabatic temperature rise.

In fact every phenol molecule cannot have more than three methylene bridges that bind it (in the configuration of maximum crosslinking) to other phenol molecules. Every bridge (formed thanks to a formaldehyde molecule) is shared by two phenol molecules, so each of these “holds” altogether three half molecules of formaldehyde (that is one and a half in total). The remaining ones are removed from the polymeric structure, after being part of it, contingently, in the resol state.

Obviously an overall generation of $(\Delta H_M + \Delta H_C)$ kcal corresponds to the formation of every methylene bridge.

Therefore an overall heat of reaction equal to $1.5 \cdot (\Delta H_M + \Delta H_C)$ is associated to every phenol mole. If we refer it to the R formaldehyde moles initially present for every phenol mole, the heat of reaction to reach the state of completely crosslinked resin turns out to be equal to:

$$\Delta H_T = (\Delta H_M + \Delta H_C) \cdot 1.5/R \quad (\text{kcal per formaldehyde mole}) \quad (1.11)$$

If on the contrary R is smaller than 1.5, the methylene bridges for each phenol molecule can be R at most, instead of 1.5 as previously seen, because a formaldehyde molecule is necessary to form every bridge. Then we will have:

$$\Delta H_T = (\Delta H_M + \Delta H_C) \cdot R/R = \Delta H_M + \Delta H_C \quad (\text{kcal per formaldehyde mole}) \quad (1.12)$$

Therefore, for instance, for $R = 2$ we have $\Delta H_T = (4.5 + 17.8) \cdot 1.5 / 2 = 16.7$ kcal/mole, while, for $R \leq 1.5$, we have $\Delta H_T = 22.3$ kcal/mole.

For reasons of steric hindrances a complete crosslinking may not be reached, in which case the actual generated heat may be smaller than ΔH_T , even if the values are however definitely higher, in all probability, than the ones (ΔH_R) corresponding to resol formation.

It is interesting, in this connection, to compare the ΔH_T values, computable as above, with the ones obtained through tests with laboratory adiabatic calorimeters.

Leung and co-workers [3] found with VSP a ΔT_{ad} of 120°C starting from 79.7 g of a reacting mixture, containing 0.678 moles of formaldehyde (n_0) and characterized by a ratio R equal to 3.26 (actually rather unusual).

With a specific heat of 0.7 kcal/kg/°C for the mixture [3;8] and a ϕ of 1.04 for the apparatus, it is easy to obtain $\Delta H = M \cdot C_p \cdot \Delta T_{ad} \cdot \phi / n_0 = 0.0797 \cdot 0.7 \cdot 120 \cdot 1.04 / 0.678 = 10.3$ kcal/mole, a value that perfectly matches the one given by formula (1.11): $\Delta H_T = (4.5 + 17.8) \cdot 1.5 / 3.26 = 10.3$ kcal/mole.

In effect the mentioned Authors just observe (without further in-depth analysis) that measured ΔT_{ad} cannot be explained if a linear polymer structure is supposed, and that therefore some crosslinking mechanism must necessarily occur.

Gustin and co-workers [1] found, still with VSP, a ΔT_{ad} of 179°C using 80 g of reacting mixture having $R = 1.89$ and containing 0.574 moles of formaldehyde.

As in this case $\phi = 1.05$, one gets $\Delta H = M \cdot C_p \cdot \Delta T_{ad} \cdot \phi / n_0 = 0.08 \cdot 0.7 \cdot 179 \cdot 1.05 / 0.574 = 18.3$ kcal/mole, a value very similar to the one given by (1.11): $\Delta H_T = (4.5 + 17.8) \cdot 1.5 / 1.89 = 17.7$ kcal/mole.

Tests performed in Italy (in 1998) with ARC (with a ϕ of about 1.6) over samples having respectively $R = 1.2$ and $R = 2.0$, even though practically unusable in order to get kinetic parameters, gave values of ΔH respectively equal to 21 and 17 kcal/mole, very similar to the values $\Delta H_T = 4.5 + 17.8 = 22.3$ kcal/mole and $\Delta H_T = (4.5 + 17.8) \cdot 1.5 / 2.0 = 16.7$ kcal/mole obtainable by (1.12) and by (1.11) respectively, that is on the basis of the above-mentioned crosslinking mechanisms.

If, in the course of adiabatic temperature rise, the reaction of resol formation did not turn into crosslinking (at temperatures higher than 140°C), but reached its completion

generating the same compounds produced in normal industrial operation, the “self-heating” curve would look like the n. 1 of fig. 7 (for ϕ close to 1).

Taking into account that curing actually happens, the true path is the one of curve n. 2, corresponding to the plot of a VSP test.

The initial part of the two curves, which is the most interesting because it includes the values useful for rupture disk sizing, is obviously coincident.

Afterwards curve n. 1 slopes down towards the value of $T_{f,R} = T_0 + \Delta T_{ad,R}$, where $\Delta T_{ad,R}$ may be evaluated through ΔH_R (the broken line is purely theoretic). On the contrary curve n. 2 goes up to $T_{f,T} = T_0 + \Delta T_{ad,T}$, where $\Delta T_{ad,T}$ corresponds to ΔH_T . If we think of the values of E and K_r obtainable from the two curves, even in a quite qualitative way, it is easy to argue that:

- activation energy is approximately the same, because, as already said, it is essentially bound to curve slope at the starting point ($T = T_0$)
- on the contrary kinetic constant is quite different, approximately in inverse proportion to ΔT_{ad} (in fact, putting $T = T_0$ in (1.8), we get $dT/dt = K \cdot x_0^{n-1} \cdot \Delta T_{ad}$; as E is practically equal and we must get the same value of dT/dt in both cases, it follows what we stated).

From the point of view of principle we might discuss which of the two curves it is fair to take into consideration.

In favour of n. 2 there is the fact that it is a completely experimental plot, and not partially “virtual”. Besides temperature $T_{f,T}$ is the one which may be actually reached, in lack of relief, in case of reaction runaway (reactor strength permitting).

In favour of curve n. 1 there is the fact that the parameters associated to it (ΔH_R , E and K_r) are the ones that most faithfully represent the reaction mechanisms that actually occur in the temperature range of practical interest.

In fact it does not look very logical that a mechanism like curing, which does not occur in the common part of the two curves, determines (through the heat of reaction that it generates) the value of the kinetic constant for that part as well!

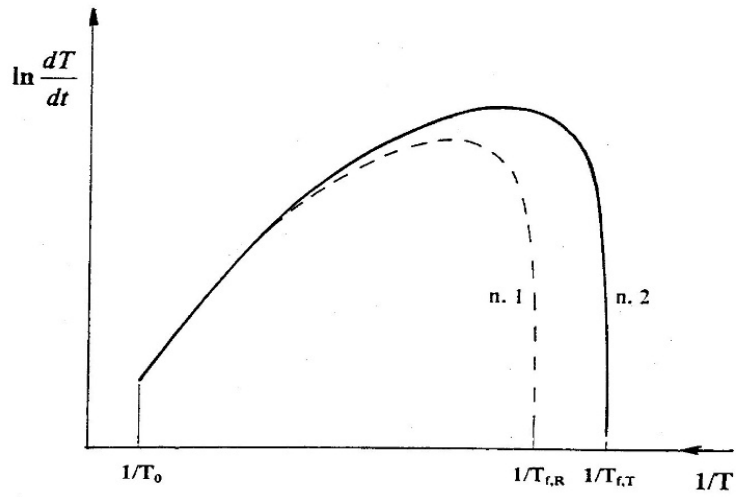


Fig. 7 – Self-heating curves in absence (n. 1) and in presence (n. 2) of crosslinking

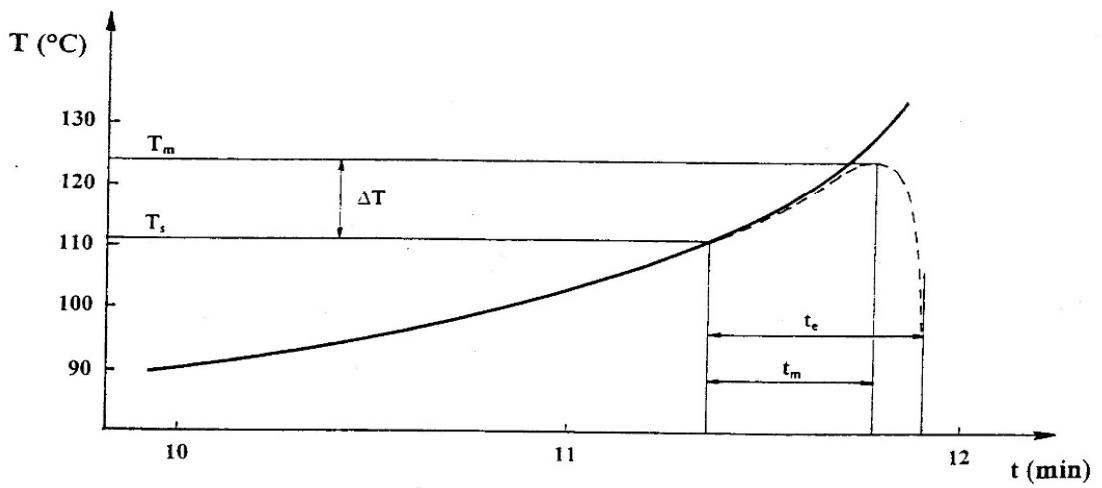


Fig. 8 – Temperature plot in venting and non-venting systems

If by chance the slope of curve n. 2 should markedly change, after the separation from curve n. 1, it would appear quite logical, as well as necessary, to rely only on curve n. 1 to get the thermo-kinetic parameters valid in the range of actual interest for our purposes.

The previous disquisition turns out to be however rather idle from a practical point of view. What matters is that the set of chosen parameters (ΔH , E and K_r) satisfies the actual path of the experimental curve describing temperature rise in the range of interest. And this is warranted by the computation procedure here suggested.

This means that, if for any reason the assumed ΔH were not correct, the value coming out for the kinetic constant would tend to compensate such an error: if we put ourselves in the condition of having to do only modest corrections to the “self-heating” curve because of a ϕ almost equal to 1 and/or of a temperature range of practical interest not much wider than the experimental one, the possible final error on thermal power generated in the relief phase will be modest as well.

It would be quite a different matter if the kinetic constant were drawn from literature data or from independent tests.

A last remark is suitable on the order of reaction. Taking into account:

- the number of actual steps that make up the overall methylation process, each with reagents (phenol and various methylolphenols) having different reactivity towards formaldehyde
- the fact that condensation reaction is influenced by catalyst concentration in a different way compared to addition
- the fact, primarily, that in condensation formaldehyde does not even intervene as a reagent,

it is clear that there is no meaning in maintaining the theoretic legitimacy of a certain order of reaction (1, 2 or others), i.e. of a certain exponent n to be associated to the concentration of the sole formaldehyde, in order to express the rate of overall reaction (addition plus condensation).

The only thing to do is to try, possibly, to interpret the overall process as a sole pseudo-reaction in which the exponent n is obtained (not necessarily as an integer) in such a way as to reproduce at best the experimental data.

1.3. EMERGENCY DISCHARGE FLUID DYNAMICS

1.3.1. Relief area calculation

At present the most used model of emission from a chemical reactor (due to a runaway reaction) is Leung model [9], based on a two-phase homogeneous exhaust flow, because it is realistic and reasonably conservative.

This model is a part of the results reached by DIERS, within the aforementioned program of studies and tests.

Taking into account that meaningful model refinements went on up to the beginning of the nineties [10;11] and that a lot of research on the matter is still in progress, it may be argued that we are dealing with a rather young technology, even if exothermic reactions have been carried out in chemical reactors for more than a century.

Actually before DIERS studies very few sources of design elements were available for sizing reactor emergency relief systems, some based on very simplistic models (that led to roughly oversized or undersized solutions), others demanding very complicated and hard to reach computer programs.

Among the most widespread sizing methods there was a diagram by FIA (Factory Insurance Association), used by insurance companies as a criterion for risk assessment in industrial plants and long since withdrawn as an official document, owing to its inadequacy and empiricism.

The chaos existing in the subject is well figured by the result of a survey by the British Plastics Federation among English manufacturers of phenolic resins [8], according to which, at the end of the seventies, the area of relief devices, related to reactor volume, varied between 0.0002 and 0.12 m²/m³, with an unjustifiable difference of over 500 times between the most and the less careful manufacturer.

Leung model assumes that liquid and gas form already inside the reactor, just before the disk rupture and also during the discharge phase, a perfectly homogeneous mixture, with an initial volumetric ratio directly correlated to the void fraction in the reactor.

The flow in the discharge duct is then assumed to be in conditions of continuous equilibrium, therefore with progressive liquid evaporation as pressure decreases along the duct.

In every instant following the rupture, the heat developed by the reaction, proportional to the mass m (kg) of liquid remaining in the reactor, goes partly to increase the temperature of that mass, partly to supply the heat of vaporization necessary to replace with vapour the space left free in the reactor by the outgoing mixture.

In figures:

$$mq = mC_p \frac{dT}{dt} + GA \frac{V}{m} \frac{\lambda}{v_g - v_l} \quad (1.13)$$

where q (kcal/sec/kg) is developed power per reacting mass unit, G (kg/sec/m²) is specific flow outgoing through the hole of area A (m²), λ (kcal/kg) is the heat of vaporization of the volatile component which determines the pressure-temperature equilibrium (water in the case of phenolic resins), V is reactor volume (m³), V/m is the specific volume of the mixture in the reactor (progressively increasing because m decreases, at constant V), v_g and v_l are specific volumes of vapour (steam in our case) and liquid (m³/kg), C_p is the specific heat (kcal/kg/°C). (*)

The expression (1.13) cannot be used if the reaction develops a gaseous component, typically noncondensable, able to affect meaningfully the relation between pressure and temperature (as it happens for instance with hydrogen peroxide decomposition).

To integrate (1.13) in an elementary way it is necessary to make some simplifying assumptions. The main one is that pressure and temperature, after disk rupture, have a moderate increase, so that C_p , λ and v_g may be considered practically constant with time. It is left to check what happens with G , m and q .

A basic feature of homogeneous two-phase flow, experimentally checked, is to give a specific mass throughput G basically constant with any change of the volumetric ratio between vapour and liquid in the reactor (and therefore even if m decreases).

(*) Actually the specific heat that appears in formula (1.13), and therefore in (1.16) and (1.17), should be (see [22]) at constant volume (C_v) and not at constant pressure (C_p), but C_v is much more difficult to determine. As in our case C_v should be about 20% lower than C_p (and therefore it would lead to a smaller rupture disk), we will conservatively use in the following the value of C_p , as usually done in the past by various authors.

As the vapour weight fraction in the discharge is minimal during the whole phenomenon (as one can easily reckon), the liquid mass flow ($-dm/dt$) is practically equal to the total flow, that is to GA . If then dm/dt is constant, it means that there is a linear decrease of m with time ($m = M - GA t$, where M is the liquid mass initially hold in the reactor).

The value of q is a function of temperature equal to $C_p(dT/dt)_p$, with $(dT/dt)_p$ got through a test in a non-venting apparatus (it is essentially the value given by (1.8) corrected to $\phi = 1$; it has nothing to do with the value dT/dt which appears in (1.13), related to a venting apparatus).

To integrate (1.13) in a simple way it is necessary to assume that q too (as C_p , G , λ and v_g) is constant with time. As this is much less true, being $(dT/dt)_p$ very sensitive to temperature variations, Leung considers a q value equal to the arithmetic mean of the two values corresponding to $T = T_s$ (temperature at disk rupture) and $T = T_m$ (highest temperature reached during discharge, unknown at the moment).

It is easy to guess, looking at (1.13), that temperature must increase at first, reach a maximum (T_m) and then drop.

In fact dT/dt is equal to the difference of two terms, of which one (q/C_p) is approximately constant with time, while the other

$$\left(\frac{GA}{C_p} \frac{V}{m^2} \frac{\lambda}{v_g - v_l} \right)$$

grows fast (because m drops).

If A is big enough, the second term is greater than the first since the beginning, and temperature starts dropping at once.

In normal situations (considering the very high A values necessary to give rise to the previous condition) dT/dt is first positive (T increases), then negative (T decreases).

Temperature drop begins certainly before the reactor is completely empty, that is when the remaining mass generates less heat than the amount taken up by the vaporization necessary to compensate for the volumetric discharge ($G \cdot V/m$), which even grows with time.

The problem is if A is great enough to contain the peak of temperature, and therefore of pressure, within smaller values than the ones corresponding to reactor strength limit.

As P and T are tied by the relation between vapour pressure of the volatile component (water in our case) and temperature, the plot of pressure against time is similar to the plot of temperature (here too there is a maximum).

In fig. 8 there is the plot of temperature against time, for a non-venting system (the same of fig. 1 with $\phi = 1$) and for a system provided with a rupture disk bursting at $T = T_s$ (broken line).

Setting in (1.13) $dT/dt = 0$ we get the value of m (which we will call m_m) for which that derivative is null (and therefore T reaches its maximum T_m):

$$m_m = \sqrt{\frac{GAV\lambda}{q(v_g - v_l)}} \quad (1.14)$$

From the expression $m = M - GA t$ we get therefore, for $m = m_m$, the time $t_m = M/(GA) - m_m/(GA)$ after which $dT/dt = 0$.

Being $M/(GA) = t_e$, i.e. the time for which $m = 0$ and therefore the reactor is completely empty, it follows that

$$t_m = t_e - \sqrt{\frac{V \cdot \lambda}{GAq(v_g - v_l)}} \quad (1.15)$$

The peak of temperature (and of pressure) is reached therefore, as qualitatively anticipated, before the reactor is empty.

Integrating (1.13), after substituting for m the expression $M - GA t$, and setting $T = T_s$ for $t = 0$, we get the plot of temperature against time after disk rupture.

Setting the further condition that $T = T_m$ for $t = t_m$ we get an explicit expression for A which is exactly the Leung formula.

$$A = \frac{Mq}{G \left[\left(\frac{V}{M} \frac{\lambda}{v_g - v_l} \right)^{1/2} + (C_p \Delta T)^{1/2} \right]^2} \quad (1.16)$$

where $\Delta T = T_m - T_s$.

In practice, once fixed T_s and T_m (the last with the method we will see), we calculate

$$q = \frac{1}{2} C_p \left[\left(\frac{dT}{dt} \right)_{ps} + \left(\frac{dT}{dt} \right)_{pm} \right] \quad (1.17)$$

and then the value of A necessary not to exceed T_m (and P_m).

If no overpressure is claimed after disk rupture ($\Delta P = 0$ and $\Delta T = 0$, with temperature and pressure immediately and progressively decreasing), the formula becomes

$$A = \frac{M^2 q (v_g - v_l)}{GV\lambda} \quad (1.18)$$

as we get directly from (1.13) with $dT/dt = 0$ for $t = 0$ (that is for $m = M$).

For the Clapeyron equation

$$\frac{\lambda}{v_g - v_l} = T \frac{dP}{dT} \quad (1.19)$$

Using for instance the three constant Antoine formula to express the relation between P and T , we have:

$$\ln P = A - \frac{B}{T + C} \quad (1.20)$$

from which

$$\frac{dP}{dT} = P \frac{B}{(T + C)^2} \quad (1.20a)$$

For computer calculations it is suitable to get A , B and C through three known couples of P and T values in the range of interest.

As we saw, the simple integration of (1.13) requires the assumption of constant values for various parameters.

Leung evaluates all of them at temperature T_s (except q).

Actually this turns out to be conservative, but subsequent elaborations always by Leung [10;11] and by Duxbury and Wilday for ICI [12] take into account average values in the range (it was soon apparent that Leung formula tended to give exceedingly conservative A values in case of large overpressures $\Delta P = P_m - P_s$).

In practice it's a question of setting $\frac{\lambda}{v_g - v_l} = \bar{T} \frac{\Delta P}{\Delta T}$ in (1.13), with $\bar{T} = \frac{T_s + T_m}{2}$

and of fixing a suitable average value for G .

Essentially identical results would be obtained using Antoine formula to calculate dP/dT and setting then

$$\frac{\lambda}{v_g - v_l} = \frac{B \bar{T} \bar{P}}{(\bar{T} + C)^2} \quad \text{with} \quad \bar{P} = \frac{P_s + P_m}{2}$$

$$\text{or} \quad \frac{\lambda}{v_g - v_l} = \left[\left(T \frac{dP}{dT} \right)_s + \left(T \frac{dP}{dT} \right)_m \right] / 2 = \frac{B}{2} \left[\frac{P_s T_s}{(T_s + C)^2} + \frac{P_m T_m}{(T_m + C)^2} \right]$$

The reliability of (1.16) becomes however uncertain in case of so high overpressures as to make $(dT/dt)_{pm}$ greater than about twice $(dT/dt)_{ps}$. (*)

It is useful, for the following remarks, to evaluate both the residual liquid fraction in the reactor (m_m/M), at the moment in which temperature and pressure reach their peak, and the time t_m at which this happens.

It is sufficient to put the value of GA given by (1.16) in the expressions (1.14) and following ones.

We get

$$\frac{m_m}{M} = 1 / \left(1 + \sqrt{\frac{C_p \cdot \Delta T^2}{\bar{T} \cdot \Delta P \cdot V/M}} \right) \quad t_e = \left[\left(\frac{V}{M} \bar{T} \frac{\Delta P}{\Delta T} \right)^{1/2} + (C_p \Delta T)^{1/2} \right]^2 / q$$

$$t_m = t_e \left(1 - \frac{m_m}{M} \right) \quad (1.21)$$

It is interesting to remark that these values, once T_s and T_m have been fixed, do not depend on G and A .

The average value \bar{m} assumed by m in the period t_m is worth

$$\bar{m} = \frac{M + m_m}{2} = \frac{M}{2} \left(1 + \frac{m_m}{M} \right) \quad (1.22)$$

Before coming to G expression, let us remark that the plot of A against P_m is a classic knee-shaped curve (fig. 9).

The beneficial influence of even moderate overpressures is apparent. Claiming that pressure does not exceed P_s after disk rupture requires relief areas, given by (1.18), even 10 ÷ 20 times larger than in the case of overpressures equivalent to about 20-50% of the absolute pressure P_s .

Obviously P_m must never exceed the reactor maximum allowable working pressure (or a value 10% higher, depending on the various codes).

(*) Actually the uncertainty is linked to the doubt whether it is permissible to use the simple expression (1.17) to evaluate q in case of high overpressures. On this subject see Appendix III.

It is better however not to rely on overpressures remarkably higher than the values corresponding to the curve knee, because small differences in the actually available area (due to incorrectly evaluated back-pressures downstream, or to inaccuracies in the method of calculating A) may cause maximum pressures much higher than expected. In brief, the beneficial effect of overpressure may be explained taking into account the time (of about some dozens of seconds) that goes by from the disk rupture to the reaching of maximum pressure.

At this moment $dT/dt = 0$ and (1.13) shows that A must be worth $\frac{m_m^2 q (v_g - v_l)}{GV\lambda}$.

As in the aforesaid time period the reactor was enabled to partially empty, m_m turns out to be equal to only a fraction of M (usually 25÷40%, as may be evaluated through (1.21)) and therefore the area A comes out to be for instance 6÷16 times smaller than in the case in which one wants the instant of maximum temperature to coincide with the starting moment (in which case obviously $m_m = M$).

However if the overpressure, and therefore the peak of temperature, are too high, then there is such an increase of q , owing to the exponential Arrhenius law that conditions $(dT/dt)_{pm}$, to almost counterbalance the factor m_m^2 and therefore prevent further remarkable drops in A .

The flat line at the base of the diagram corresponds to the assumption of emission of vapour alone through the broken disk, owing to a perfect liquid/vapour disengagement (which is normally an unrealistic hypothesis in the case of chemical reactors).

The A value obtainable under this assumption is much smaller, because the specific volumetric flow that passes through the disk is much higher than in two-phase conditions.

On the other hand, as there is no substantial decrease of reacting mass during the discharge phase (m changes very little with time, owing to vaporization alone), overpressure turns out to have no appreciable beneficial effect.

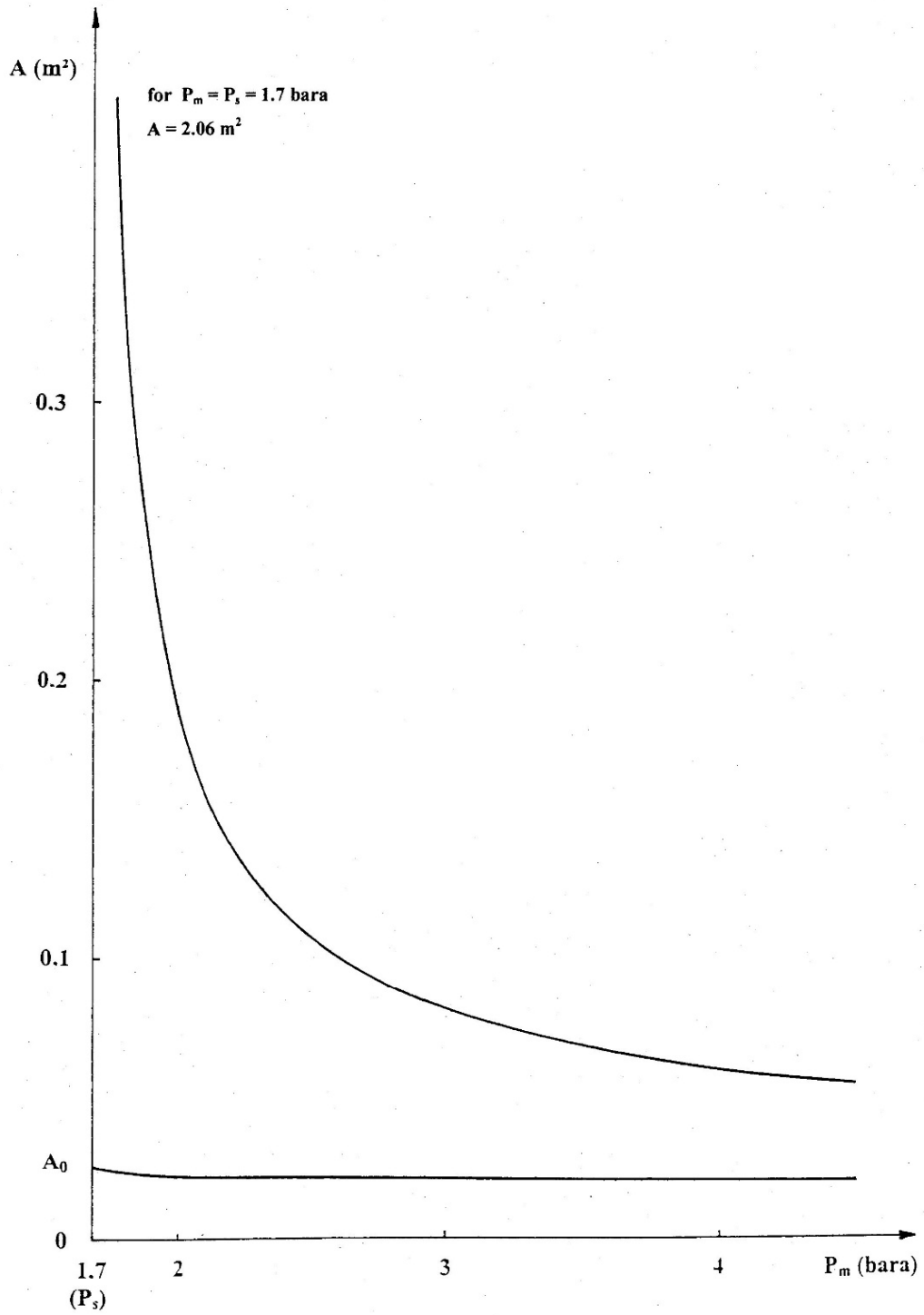


Fig. 9 – Vent area versus maximum pressure

The expression that gives the value of A against P_m may be got even in this case through (1.13), only replacing V/m with v_g . Integration leads, paradoxically, to a more complicated expression, of transcendental type, from which A cannot be got in explicit form as in (1.16).

On the other hand the flat plot implies that the only really interesting value of A is the one (A_0) for $P_m = P_s$. This value may be obtained directly from (1.13), modified as said before, setting $dT/dt = 0$ for $t = 0$ (that is for $m = M$).

We get:

$$A_0 = \frac{Mq(v_g - v_l)}{Gv_g\lambda} \quad (1.23)$$

1.3.2. Two-phase flow calculation

Up to the end of the eighties it was necessary to apply to sophisticated computer programs for evaluating discharge capacity in two-phase flow conditions.

The fundamental merit of Leung, beyond the formula (1.16), is the elaboration [13;21] of a theory of homogeneous two-phase flow, in equilibrium conditions (HEM, that is Homogeneous Equilibrium Model), able to give G on the basis of simple formulas.

The equation of state assumed and used for discharge calculations is the following:

$$\frac{v}{v_0} - 1 = \omega \left(\frac{P_0}{P} - 1 \right) \quad (1.24)$$

where v is the specific volume (m^3/kg) of the two-phase mixture in a generic point (with pressure P) of the discharge duct, while the values v_0 and P_0 are related to the “calm” area at the duct entrance.

The fundamental parameter ω , as it is apparent in the form $\omega = \left(\frac{v-v_0}{v_0} \right) / \left(\frac{P_0-P}{P} \right)$, expresses the property of the mixture to expand in percentage its volume with reference to a certain relative pressure decrease.

It turns out to be based only on the physical-geometrical properties prevailing in the aforesaid calm area:

$$\omega = \alpha \cdot \left(1 - 2P \frac{v_g - v_l}{\lambda} \right) + \frac{C_p T P}{v} \cdot \left(\frac{v_g - v_l}{\lambda} \right)^2 \quad (1.25)$$

where α is the vapour volumetric fraction in the inlet section (in the previous expression the 0 subscript has been omitted for simplicity in the various parameters, which refer all however to the conditions prevailing in the calm area).

ω parameter is made up of two distinct terms: the first reflects the expansibility of the mixture due to the existing vapour volumetric fraction, the second regards the expansibility due to the phase change upon depressurization.

If the reactor content goes to make up, all along the discharge phase, a homogeneous two-phase mixture, then α will be equal to the void fraction in the same reactor $(1 - mv_l/V)$ and v will be equal to V/m . Besides the first term of ω comes out to be much smaller than 1 and practically negligible in comparison with the second (which usually is worth 10÷40).

If at the top of the reactor a perfect liquid/vapour disengagement could be assumed, then α would become equal to 1 and v to v_g .

In this case the second term (and not the first as before) would be almost negligible (take into account that the previous equation of state still holds, with good approximation, even in the limit case of a fluid made up of pure vapour).

In the first hypothesis of two-phase flow, more interesting for us, ω expression becomes (applying Clapeyron relation):

$$\omega = \left(1 - \frac{mv_l}{V}\right) \left(1 - 2 \frac{P}{T} \frac{dT}{dP}\right) + \frac{m}{V} C_p \frac{P}{T} \left(\frac{dT}{dP}\right)^2 \quad (1.26)$$

Prevailing conditions in the reactor, which determine the value of the various parameters in ω expression, change however with time, during the discharge period.

Therefore it is convenient to refer, as already done in the previous paragraph, to average values assumed between the starting moment and the one corresponding to the maximum pressure. We have then:

$$\bar{\omega} = \left(1 - \frac{\bar{m}v_l}{V}\right) \left(1 - 2 \frac{\bar{P}}{\bar{T}} \frac{\Delta T}{\Delta P}\right) + \frac{\bar{m}}{V} C_p \frac{\bar{P}}{\bar{T}} \left(\frac{\Delta T}{\Delta P}\right)^2 \quad (1.27)$$

where \bar{m} , \bar{P} and \bar{T} were already defined and calculated in the previous paragraph.

Reactor discharge usually takes place in critical flow condition. If the relief device has the shape of a frictionless nozzle, the critical ratio η_{oc} (between critical pressure and upstream pressure, i.e. in the reactor) is much greater than the classic one for gases and vapours.

For two-phase flow η_{oc} is approximately equal to 0.9, while for perfect gases the classic theory gives

$$\eta_{oc} = \left(\frac{2}{k+1}\right)^{\frac{k}{k-1}} \quad (1.28)$$

where k is the ratio between specific heats at constant pressure and volume.

For superheated steam, comparable to a perfect gas, it is $k = 1.31$ (for temperatures of 100÷200°C) and therefore $\eta_{oc} = 0.544$.

For saturated steam (that is in the most interesting conditions for us) the previous expression still holds considering for k the value 1.135, that leads to $\eta_{oc} = 0.577$.

According to ω method we have (as better explained in Appendix I):

$$\eta_{oc} = 0.6055 + 0.1356 \ln \omega - 0.0131 \ln^2 \omega \quad (1.29)$$

Then

$$\frac{G_{oc}}{\sqrt{P/v}} = \frac{\eta_{oc}}{\sqrt{\omega}} \quad (1.30)$$

where G_{oc} is the specific flow (kg/sec/m²) in critical conditions.

For $\omega = 0.88$ (corresponding approximately, as we will see in the following, to the typical value for saturated steam) we have $\eta_{oc} = 0.59$, a result very similar to the one given by classic theory.

Coming back to the case of two-phase flow, (1.30) becomes, in terms of average values to be used later on in calculations:

$$\frac{\overline{G_{oc}}}{\sqrt{\overline{P} \overline{m}} \overline{V}} = \frac{\overline{\eta_{oc}}}{\sqrt{\overline{\omega}}} \quad (1.31)$$

where $\overline{\eta_{oc}}$ is the value of η_{oc} calculated for $\omega = \overline{\omega}$ and $\overline{G_{oc}}$ is the average value of G_{oc} .

As $\eta_{oc} \approx 0.9$, from (1.30) we can get (disregarding the first term in ω):

$G_{oc} = 0.9 \frac{dP}{dT} \left(\frac{T}{C_p} \right)^{1/2}$ which reminds of the formula $G_{oc} = \frac{dP}{dT} \left(\frac{T}{C_p} \right)^{1/2}$ used for two-phase flow within other simplified models (for instance ERM by Fauske).

Using Antoine formula for the relation between P and T , we get:

$$G_{oc} = 0.9 \frac{PB}{(T + C)^2} \left(\frac{T}{C_p} \right)^{1/2}$$

from which it turns out that G_{oc} is approximately proportional to $P/T^{1.5}$, but it does not depend basically on m/V .

This is an important result, because it confirms the hypothesis made in the previous paragraph of considering a constant mass flow during discharge, in spite of the remarkable m drop.

P and T show smaller changes, taken enough into account considering, in $\overline{G_{oc}}$ evaluation, the average \overline{P} and \overline{T} values.

Notice, besides, that what said before means that, in order to evaluate $\overline{G_{oc}}$, considering \overline{m} or even M as the value for m leads practically to the same result.

The previous formulas for η_{oc} and G_{oc} hold in the case of discharge through frictionless nozzles.

But usually downstream the rupture disk there is a conveying pipe with a diameter D , a certain length L and a certain number of bends. Therefore it is necessary to take into account the additional resistance involved, which further limits the flow G (we will name L_e the equivalent pipe length, that is the one that, for pressure drop evaluation, takes into account also elbows and other localized resistances).

We will set

$$G = C_c \cdot G_{oc} \quad \text{and, as an average value,} \quad \bar{G} = C_c \cdot \overline{G_{oc}} \quad (1.32)$$

The reduction coefficient C_c depends on three parameters:

- ω (already seen)
- $N_t = 4fL_e/D$, the flow resistance factor, equal to the number of velocity heads corresponding to pressure losses (if we choose conservatively $f = 0.005$ for the Fanning friction factor, according to Leung's advice, it turns out that a velocity head is lost every 50 diameters of pipe length; it is then necessary to add, for getting N_t , $N = 0.5$ for a square cut pipe entrance, $N = 1$ for a *Tee* fitting, $N = 0.25$ for a long-radius 90° elbow, $N = 0.15$ for a long-radius 45° elbow, $N = 0.05 \div 0.3$ for a burst disk, etc.)
- $Fi = \frac{mgH}{VN_tP} \quad \left(\bar{F}i = \frac{\bar{m}gH}{VN_tP} \text{ as an average} \right) \quad (1.33)$

which is a modified Froude number, where g is the gravitational acceleration and H the height difference, positive or negative, between the pipe outlet and inlet (as the density of two-phase flow is much closer to the liquid than to the vapour density, hydrostatic head has a controlling influence).

The value of C_c is a very complex analytical function of the three aforesaid parameters [6].

In Appendix I we report the rigorous method for calculating it, together with a table of numerical values. We also give approximate expressions which allow C_c evaluation with adequate accuracy in the range of the most usual values of the three parameters at stake.

Such expressions should allow easier calculations, especially for computer applications, in comparison with design charts available in literature [14].

The actual critical ratio η_c changes, owing to the pipe presence. We have:

$$\eta_c = C_c \cdot \eta_{oc} \quad \text{and, as an average value,} \quad \overline{\eta_c} = C_c \cdot \overline{\eta_{oc}} \quad (1.34)$$

Therefore it is necessary to check, in order to satisfy the hypothesis of critical conditions on which the expressions for G_{oc} and G are based, that $P_a / P_s < \overline{\eta_c}$ (P_a is the pressure in the discharge environment for reactor outflow).

Notice that, owing to (1.32) and (1.34), expression (1.30) turns into:

$$\frac{G}{\sqrt{P/v}} = \frac{\eta_c}{\sqrt{\omega}} \quad (1.35)$$

The formulas in this and in the following paragraph can be used for the calculation of rupture disks as well as of safety valves.

These valves are seldom used in the phenolic resins field, especially for the great trend to scaling and clogging of these resins.

In Appendix II we report however, for completeness, the method for sizing valves and relevant piping, in order to better point out the differences with disks calculations.

1.3.3. Thrust calculation

We mention here the method of calculation of the thrust T produced by the two-phase flow in the discharge pipe. This thrust is present in every point of the pipe and is direct along its axis and against the flow direction.

This calculation is necessary to size the pipe supports and to check for instance the stresses generated, in the point of connection of the pipe to the reactor, principally by the bending moment equal to T multiplied by the arm that comes out.

From the application of momentum theorem we get

$$T = A_p(G^2 \cdot v_e + P_e - P_a)$$

where subscript e refers to conditions at pipe outlet, P_a is the pressure in the discharge environment, A_p is the duct inner section.

Conditions at pipe end may be either subcritical ($P_a > P_c$), in which case $P_e = P_a$ and $v_e = v_a$, or critical ($P_a < P_c$) and then $P_e = P_c$ and $v_e = v_c$.

In the first case we get

$$\frac{T}{P_0 A_p} = \frac{v_a}{v_0} \cdot \frac{G^2 v_0}{P_0} \quad (1.36)$$

In the second case (the usual one) we get on the contrary

$$\bar{T} = \frac{T}{P_0 A_p} + \frac{P_a}{P_0} = \frac{G^2 \cdot v_0}{P_0} \cdot \frac{v_c}{v_0} + \eta_c \quad (1.37)$$

In both cases subscript 0 refers to conditions inside the reactor, while $\eta_c = P_c/P_0$ is the critical ratio already defined and \bar{T} is the so called thrust coefficient (whose value, in the case of critical conditions at pipe end, turns out to be independent on P_a/P_0).

Since we have, owing to the state equation (1.24) and to (1.35),

$$\frac{v_c}{v_0} = 1 + \omega \left[\frac{1}{\eta_c} - 1 \right] \quad \frac{G^2 \cdot v_0}{P_0} = \frac{\eta_c^2}{\omega}$$

from (1.37) we get at last

$$\bar{T} = \left(\frac{1}{\omega} - 1 \right) \eta_c^2 + 2\eta_c \quad (1.38)$$

However, DIERS [14] recommends to take into account, in η_c evaluation, only head losses through pipe entrance ($N = 0.5$ if square cut) and burst disk ($N = 0.3$ at most), disregarding the contribution of downstream pipe.

There are indeed some transient reaction forces, which develop in the initial instants immediately after disk burst, not taken into account by usual steady-state calculations. Such reaction forces are basically equal to the steady-state ones in the case of short pipes, while they are much higher in the case of long ducts (these involve a high N_t , and therefore η_c and eventually \bar{T} turn out to be low). Hence the advisability of taking into no account the piping downstream the disk.

That means to consider $N_t = 0.8$ and $Fi = 0$, getting a C_c value (typically for $\omega = 10 \div 40$) equal to about 0.88 (see Appendix I). Being then $\eta_{oc} = \sim 0.9$ (for the same ω values), it comes out $\eta_c = \sim 0.8$ and $\bar{T} = \sim 1$, which is an approximation more than acceptable, taking into account the conservative simplifications already introduced (a more exact calculation carries \bar{T} values variable from 0.983 for $\omega = 10$ to 0.986 for $\omega = 40$).

We get then $T = (P_0 - P_a) \cdot A_p$, which means (if P_a is approximately equal to atmospheric pressure) that thrust load is equivalent to the action, on the inner pipe section, of the maximum gage pressure reached inside the reactor (in fact it is logical, for calculation purposes, to consider P_0 equal to P_m , that is to the maximum reactor pressure during discharge).

To take into account the unavoidable dynamic effects associated with time-dependent loads, DIERS recommends to apply a safety factor of 2 to the thrust as above determined.

In the case of emission of a pure vapour the treatment of the subject is the same and expression (1.38) still holds.

For $\omega = 0.88$ (saturated steam), (1.29) gives $\eta_{oc} = 0.59$. Considering also here $N_t = 0.8$, we get (for $\omega = 0.88$) $C_c = 0.82$ (see Appendix I) and then $\eta_c = 0.82 \cdot 0.59 = 0.48$ and $\bar{T} = \sim 1$, that is the same result as in two-phase flow conditions.

1.3.4. Identifying the flow conditions

In the previous paragraphs we said that the Leung model is based upon conditions of homogeneous two-phase flow, which are both more conservative than those relevant to other possible models and fairly corresponding to what actually happens in chemical reactors.

In presence of bubbles generation inside a liquid mass, owing to boiling or to a gaseous reaction product, the mass itself swells up and, with large enough vapour flows, it can reach the level of the discharge nozzle. A two-phase outgoing flow is then generated, instead of a simple vapour emission.

The onset of this phenomenon depends not only on the gaseous flow rate, but also on the degree of filling of the reactor and on the type of the reactive mixture.

If this has a poor tendency to foaming, we have a so called “churn-turbulent” behaviour (with large and irregular bubbles), while if the tendency is great we have a “bubbly” regime (with fine bubbles), which in its extreme version corresponds to the “homogeneous” model.

Passing from the first to the last case we have a greater and greater liquid swelling; therefore two-phase flow begins at lower and lower vapour flow rates and degrees of filling.

Besides, while in the “churn-turbulent” regime we have, after the onset of the two-phase flow, a certain disengagement between liquid and vapour (so the liquid fraction in the outgoing flow is smaller than the average one inside the reactor), in the “homogeneous” case, as already seen, the outgoing two-phase mixture is considered to have the same composition as the perfectly mixed mixture contained in the reactor. It is possible, besides, that the emission begins in the two-phase regime and then, at a certain degree of voiding, tends to get all-vapour venting. Depressurization then goes on, as already mentioned, much faster.

Leung himself [15] got some formulas to calculate vent areas in “churn-turbulent” and “bubbly” conditions. In both cases, but especially in the first, smaller values are obtained in comparison with the “homogeneous” model.

The characterization of a reactive mixture, to ascertain to which category it belongs, can be done only experimentally (for instance through VSP apparatus). However,

DIERS deems it imprudent to base calculations on models less conservative than the homogeneous one, considering that minimum compositions variations may be sufficient to change the type of behaviour.

The following example may be quoted to the purpose.

A 2" vent nozzle was suddenly opened on a 2 m³ vessel, 95% full of tap water at 150°C and at the corresponding saturation pressure: about 28% of the content was vented in two-phase regime.

The experiment was repeated, after adding 1000 ppm of a domestic detergent to water: 96% of the content was vented, with a clearly different mechanism of two-phase flow. It is then necessary to take into account that a lot of reactive mixtures (for instance styrene-polystyrene) show a "homogeneous" behaviour, even if they do not form a stable foam when shaken or agitated.

DIERS' quantitative methods for predicting whether or not a reactive system will undergo two-phase venting are the following.

- 1) We calculate vapour superficial velocity J (m/sec)

$$J = \frac{W}{\rho_g A_r}$$

where W (kg/sec) is the flow rate of vapour, having density ρ_g (kg/m³), in the reactor with section A_r (m²)

- 2) We calculate the velocity of bubble rise U_b (m/sec)

$$U_b = K_b \left[\frac{g\sigma(\rho_l - \rho_g)}{\rho_l^2} \right]^{1/4}$$

where $g = 9.81$ m/sec², σ (N/m) is the liquid surface tension, ρ_l and ρ_g (kg/m³) are liquid and vapour densities. K_b is a constant equal to 1.53 for "churn-turbulent" regime and 1.18 for "bubbly" regime

- 3) We then calculate the dimensionless vapour superficial velocity $\psi_F = J/U_b$ and compare it with the one (ψ) at which two-phase flow begins.

If $\psi_F \geq \psi$ we just have two-phase flow.

If $\psi_F < \psi$ we have all-vapour venting (or we have complete disengagement and all-vapour emission if we had before $\psi_F \geq \psi$ and therefore two-phase conditions)

- 4) The discriminating value ψ is given by (α is the void fraction in the reactor):

- in “churn-turbulent” regime:

$$\psi = \frac{2\alpha}{1-C_0\alpha} \quad \text{with } C_0 = \begin{matrix} 1.5 \text{ best estimate} \\ 1 \text{ conservative} \end{matrix}$$

- in “bubbly” regime:

$$\psi = \frac{\alpha(1-\alpha)^2}{(1-\alpha^3)(1-C_0\alpha)} \quad \text{with } C_0 = \begin{matrix} 1.2 \text{ best estimate} \\ 1.01 \text{ conservative} \end{matrix}$$

($C_0 = 1.01$ corresponds to the homogeneous regime)

Coming to a practical example, let us consider the reaction between phenol and formaldehyde in aqueous solution, at a temperature of 100°C.

Let us assume $\sigma = 56.6 \cdot 10^{-3}$ N/m, which is practically the surface tension of water (as reported in [8] by British Plastics Federation). Being $\rho_l = 1100$ kg/m³ and $\rho_g = 0.598$ kg/m³ (it is the density of saturated steam at 100°C), we get $U_b = 0.177$ m/sec in “bubbly” regime and $U_b = 0.229$ m/sec in “churn-turbulent” regime. These values, besides, change very little with temperature and pressure (σ is worth $63 \cdot 10^{-3}$ N/m at 75°C and $52.5 \cdot 10^{-3}$ N/m at 125°C).

Assuming $\alpha = 0.242$ (corresponding to 15,000 kg of reactive mixture with $\rho_l = 1100$ kg/m³ in a 18 m³ reactor) we get:

- in “churn-turbulent” regime $\psi = 0.76$ (with $C_0 = 1.5$)
- in “bubbly” regime $\psi = 0.20$ (with $C_0 = 1.2$)
- in “homogeneous” regime $\psi = 0.19$.

The maximum allowable vapour velocity (J_{max}), to avoid two-phase flow, is equal to $\psi \cdot U_b$ and therefore to $0.76 \cdot 0.229 = 0.174$ m/sec in the most optimistic case (“churn-turbulent” regime) and to $0.19 \cdot 0.177 = 0.0336$ m/sec in the most pessimistic case, i.e. in that homogeneous regime which is usually considered the most realistic for the reaction between phenol and formaldehyde.

The thermal power corresponding to velocity J_{max} , considering a vaporization heat λ of 540 kcal/kg and a reactor section of 5 m², is worth

$$Q = \lambda \cdot J_{max} \cdot A_r \cdot \rho_g \cdot 3600 = 540 \cdot 0.0336 \cdot 5 \cdot 0.598 \cdot 3600 = 195,000 \text{ kcal/h}$$

in homogeneous regime (or 1,011,000 kcal/h in “churn-turbulent” regime).

Whoever operates a phenolic reactor with a reflux condenser will find absurdly small the value of 195,000 kcal/h, as he is used to dealing every day with quite higher thermal

fluxes (even higher than those allowable in churn-turbulent regime) with no remarkable swelling of the reactive mass and no liquid entrainment into the tube bundle.

For the same reactor of the previous example the plot of temperature against time was recorded during a normal production cycle.

The rising velocity of temperature (dT/dt) just before 100°C, i.e. the beginning of mass boiling, turned out to be equal to 2.1°C/min.

This means a thermal power, excluding the fraction absorbed by cooling water in jacket and inner coil, equal to

$$Q = M \cdot C_p \cdot dT/dt = 15,000 \cdot 0.7 \cdot 2.1 \cdot 60 = 1,323,000 \text{ kcal/h}$$

This power turns suddenly (as soon as temperature rise stops, at 100°C) into mass vaporization heat, which goes to be disposed of, with no problem, in the reflux condenser.

The experimental value is therefore even larger than the maximum foreseen (without entrainment) by the “churn-turbulent” model.

Moreover, in anomalous operating conditions, temperature rising rates up to about 3 °C/min (at 100 °C) have been recorded, with no apparent impairment of condenser efficiency and no harmful effect.

On the other hand DIERS’ approach to this subject is certainly very conservative, as pointed out by Wallis himself (1984), whose works had been used by DIERS to arrive at the expressions of U_b and ψ above reported.

The reason for this discrepancy seems to be due to the fact that bubbles generated in the transient “flashing” phenomena are much bigger and faster in rising than the ones used in the experiments of gaseous bubbling from which Wallis’ results came out. Therefore these results could not be applied as such to the cases examined by DIERS. The above statements do not compromise however the validity of the sizing formulas for vent areas previously reported, because the vapour flows generated in emergency situations are quite larger than the minimum ones necessary for the onset of two-phase flow.

2. DESCRIPTION OF EXPERIMENTAL TESTS

2.1. THE PILOT APPARATUS

The small reactor used for our tests was built for the purpose with the following features:

- material: stainless steel sheet 1 mm thick
- shape: vertical cylinder (250 mm diameter, 300 mm height, with a gross capacity of 14.7 litres)
- insulation of side wall, bottom and cover (built with a removable half for mixer insertion) by means of 50 mm of ceramic wool, with relevant containment sheet
- small powered propeller mixer, with variable speed
- thermocouple with measuring tip in direct contact with the liquid, connected to a temperature recorder with 0÷100°C range
- feed tube to insert catalyst and quench water.

Reactor was filled with 5 kg of reactive mixture with various compositions, so as to leave an adequate space for quench water.

On the basis of masses and specific heats of the various materials at stakes (3 kg and 0.12 kcal/kg/°C for stainless steel; 0.7 kcal/kg/°C [8] for the reactive mixture) we calculated with (2.4) a ϕ equal to 1.10.

For evaluating residual heat losses, in order to take account of them in calculations, we put 5 litres of boiling water in the agitated reactor and we recorded the plot of temperature decrease against time down to 60°C.

The accuracy of recorder markings was controlled comparing them with the direct readings of a mercury thermometer.

For measurement of quench water, fed by gravity into the reactor, we used a transparent and graduated cylindrical container of about 12 litres, connected to the reactor through a small hose with inlet valve.

The removable half of the cover was simply supported on a gasket, so as to give no resistance to possible overpressures. For safety reasons and to avoid possible overflowing, the reactor was placed into a small containment basin.

2.2. PERFORMED TESTS

We performed various tests, each with the following procedure:

- separate preparation of reagents quantities necessary to overall make 5 kg of mixture (having 1.10 density) according to the various planned recipes
- heating of reagents in a bain-marie up to the wanted temperature T_0 of reaction onset (60÷75°C)
- pouring of reagents into the reactor with open cover, closing of the vessel and starting of the recorder
- catalyst insertion (30% caustic soda solution) through proper tube
- recording of temperature rise in adiabatic conditions, up to 99°C
- quench water feeding in a measured and progressive way, through intermittent opening of the proper valve, so as to keep the temperature of reacting mass between 95 and 99°C
- carrying on the reaction up to temperature stabilization at about 98°C with no more need of water additions, i.e. up to almost complete formaldehyde consumption
- quick mass quenching with water until temperature drop to the initial T_0 value.

The value of T_0 was suitably chosen every time so that the initial temperature rising rate, due to chemical reaction, would be definitely higher than the falling rate due to heat losses.

In the following table we report, for two of the performed tests, the initial concentrations of formaldehyde and caustic soda, the temperature T_0 of reaction onset, the time to rise from T_0 to 99°C in adiabatic conditions, the residence time at 95÷99°C (with progressive additions of quench water) in order to complete the reaction of resol formation.

More exactly the reported temperature T_0 is the one recorded just after the sudden initial rise due to the heat of soda solubilization and of phenol salification.

Such increase was of about 1.5°C with the normal catalyst dose (test n. 1) and 4°C with the larger dose (test n. 2).

To keep under control at 95÷99°C the reaction temperature it was necessary to add to the reacting mass 4.5÷5 litres of water at 18÷20°C.

As many litres were added to lower the temperature by about 30°C at the end of the reaction.

Table 1

Test N°	X_{0,form} (moles/l)	X_{NaOH} (moles/l)	T₀ (°C)	t rise (min)	t reaction (min)
1	9.88	0.112	67	10.7	90
2	9.59	0.350	61	5	45

3. GETTING THE THERMOKINETIC PARAMETERS

3.1. TESTS WITH PILOT REACTOR

We will describe in detail the procedure for getting the various thermokinetic parameters from the two tests above quoted.

In fig. 10 we find the recording of the temperature rise plots. In abscissa there are the times, in ordinate the temperatures.

In table 2 we find, for different values of temperature, the values of the slope of the curves in fig. 10 (dT/dt in °C/min), both as directly taken from the curves and corrected for heat losses.

In this connection, from the experimental plot of temperature drop against time, with a load of 5 kg of boiling water in the agitated reactor, we got between 60 and 100°C a value for dT/dt in °C/min, due to heat losses, approximately equal to

$$\left(\frac{dT}{dt}\right)_{H_2O} = 0.0073 \cdot (T - 52) \quad \text{with } T \text{ in } ^\circ\text{C}$$

Modified for an equal quantity of reactive mixture, which has $C_p = 0.7$ kcal/kg/°C, this expression becomes

$$\frac{dT}{dt} = 0.0104 \cdot (T - 52)$$

which gives the values of made corrections.

Table 2 (dT/dt in °C/min)

Test n. 1										
T (°C)	67	70	73	76	79	82	86	90	94	98
(dT/dt) _{read}	1.36	1.54	2.08	2.57	2.96	3.75	4.63	5.56	7.33	8.67
(dT/dt) _{corrected}	1.52	1.73	2.30	2.82	3.25	4.07	4.99	5.96	7.77	9.16
Test n. 2										
T (°C)	62	66	70	74	78	82	86	90	94	98
(dT/dt) _{read}	3.07	4.29	5.88	7.50	9.71	12.3	15.5	19.5	23.0	31.0
(dT/dt) _{corrected}	3.18	4.44	6.07	7.73	9.98	12.6	15.9	19.9	23.4	31.5

For the calculation of the heat of reaction we went on as follows.

In the case of test n. 1 it was necessary to add 4.5 litres of water at 19°C to keep under 100°C the reaction temperature and 5.0 more litres to fall again to the starting temperature of 67°C.

The calories overall developed by the reaction are therefore those corresponding to heating 9.5 kg of water from 19 to 67°C, i.e. $9.5 \cdot (67 - 19) = 456$ kcal.

To these we must however add the calories corresponding to the heat dispersed in air by mass M , which remained at an average temperature of 95°C for a time $t_r = 100$ minutes. This loss may be evaluated using the same formula previously found, through the expression

$$M \cdot C_p \cdot dT/dt \cdot t_r = 5 \cdot 0.7 \cdot 0.0104 \cdot (95 - 52) \cdot 100 = 157 \text{ kcal}$$

Overall heat generated by the reaction was equal to $456 + 157 = 613$ kcal.

Being 44.9 the formaldehyde moles contained in 5 kg of reactive mixture ($9.88 \cdot 5 / 1.1$), the heat of reaction turns out to be equal to $613/44.9 = 13.7$ kcal/mole.

In the case of test n. 2 we added 5.0 litres of water at 20°C to keep under control the reaction temperature and 5.0 more litres to fall again down to 68.5°C (it was impossible to reach the initial temperature of 61°C to avoid liquid overflowing from the reactor).

Heat losses in air, with reacting mass at an average temperature of 97°C for 50', were equal to

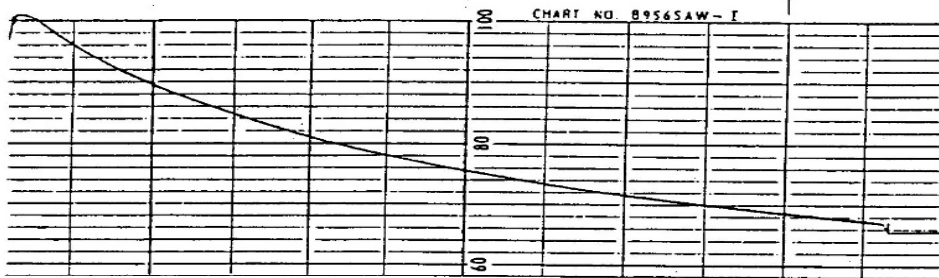
$$5 \cdot 0.7 \cdot 0.0104 \cdot (97 - 52) \cdot 50 = 82 \text{ kcal}$$

Overall heat generated by the reaction was equal to these losses, plus the calories necessary to heat from 20 to 68.5°C 10.0 kg of water (i.e. 485 kcal), plus the calories necessary to heat 5 kg of mixture and 3 kg of reactor metallic mass from 61 to 68.5°C, i.e. $(5 \cdot 0.7 + 3 \cdot 0.12) \cdot (68.5 - 61) = 29$ kcal.

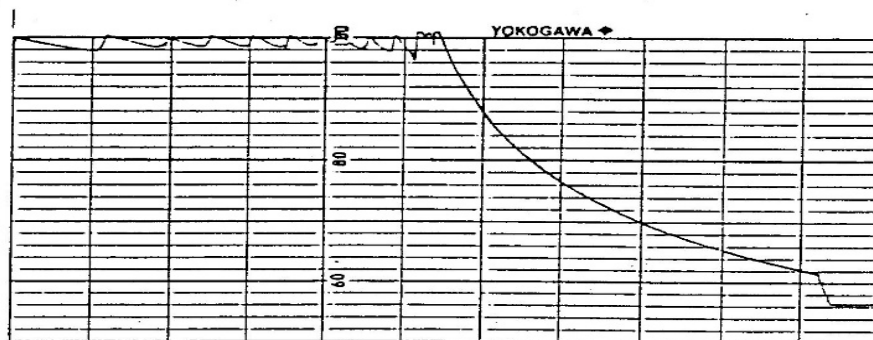
Overall it means $82 + 485 + 29 = 596$ kcal which, related to 43.6 moles of formaldehyde contained in 5 kg of this reactive mixture, are equivalent to a heat of reaction of 13.7 kcal/mole.

In the previous heat balances we implicitly disregarded the presence of possible mixing heats (rather unlikely) between water and reacting mass.

As noticeable from calculations, the influence of heat losses (difficult to evaluate correctly) on the value of ΔH is somewhat remarkable in the case of test n. 1.



Test n. 1



Test n. 2

Fig. 10 -- Records of adiabatic temperature rises.
 Temperatures (°C) in ordinate, times (1 cm = 1 min) in abscissa.

For test n. 2 (which lasted much less owing to the large quantity of added catalyst) the influence of heat losses turned out to be much more moderate, and the fact that the obtained value is equal to the one of test n. 1 (as it must be) is an implicit and encouraging validation of the way we took losses into account.

Once we got thus the ΔH values, we have, as seen in par. 1.1.1 (expression 1.6),

$$\Delta T_{ad,\phi} = \frac{\Delta H \cdot V_l \cdot x_0}{M \cdot C_p \cdot \phi} = \frac{\Delta H \cdot n_0}{M \cdot C_p \cdot \phi}$$

where n_0 is the number of initial moles of formaldehyde. We then calculate $T_{f,\phi} = T_0 + \Delta T_{ad,\phi}$.

For instance for test n. 1 we get (expressing temperatures in °K)

$$\Delta T_{ad,\phi} = \frac{13.7 \cdot 44.9}{5 \cdot 0.7 \cdot 1.1} = 160^\circ\text{K} \quad T_{f,\phi} = 67 + 273 + 160 = 500^\circ\text{K}$$

For test n. 2 we get in the same way $\Delta T_{ad,\phi} = 155^\circ\text{K}$ and $T_{f,\phi} = 489^\circ\text{K}$.

Now it is necessary to calculate, for every test, $\ln[(dT/dt)/(T_{f,\phi} - T)^n]$ as a function of $1/T$, using the above found value of $T_{f,\phi}$ and the values of T (changed into °K) and of $(dT/dt)_{correct}$ in °K/min from table 2.

Calculations must be performed for various n values, so as to find for which of them the set of experimental points lays down along a straight path.

Actually, in our case, we get a good alignment both with $n = 1$ and with $n = 1.5$ or 2 .

This is due to the fact that the set of available points extends up to a temperature corresponding to a rather limited degree of formaldehyde conversion: only at much higher conversion levels (however outside the range of our interest) the trend of interpolating lines would become appreciably different when n changes.

In practice that means that, for the purposes of safety studies, it is all the same which n value is chosen in the range $1 \div 2$. According to the choice the consequent values of the other parameters (E and K_r) will obviously change, but the path of the experimental curve $T = T(t)$ will be however faithfully followed.

Nevertheless we chose $n = 1.5$ because it leads to results, in terms of residual formaldehyde concentrations towards the end of the reaction of resols formation, which more faithfully reflect the experimental values supplied by the technicians of this industrial sector.

Thus the parameters obtained with this procedure turn out to be applicable also to the analyses of process operation and productivity, besides to safety analyses.

In fig. 11 we report, for the two tests, the values of $\ln \left[(dT/dt)/(T_{f,\phi} - T)^{1.5} \right]$ against $1/T$, with the two interpolating straight lines.

As one can notice, the various points turn out to be well aligned along an almost perfectly straight path: the statistical regression analysis gives an absolute value of 0.999 for the correlation coefficient r in both cases. That means that considering the overall reaction of resols formation as a single elementary pseudo-reaction of order 1.5, with velocity and degree of completion correlated to the concentration of the sole formaldehyde, is a valid working hypothesis (or simulation).

Besides it is reasonable to deem that extrapolating up to T values moderately higher than 100°C is a sufficiently reliable operation.

The slopes of the two straight lines give directly the value of E/R .

The ordinate y_r of the line, in correspondence of $1/T = 1/T_r$ (we assume $T_r = 373^\circ\text{K}$, i.e. 100°C , as the reference temperature), gives the value of K_r .

More exactly we have (taking account of expression 1.8)

$$K_r \sqrt{\frac{x_0}{\Delta T_{ad,\phi}}} = e^{y_r}$$

For test n. 1 we get $E/R = 8750^\circ\text{K}$, from which $E = 8750 \cdot 1.987 \cdot 10^{-3} = 17.4$ kcal/mole.

Besides $y_r = -4.917$ and $x_0 = 9.88$ moles/l, from which

$$K_r = 7.32 \cdot 10^{-3} \cdot \sqrt{\frac{160}{9.88}} = 2.95 \cdot 10^{-2} \text{min}^{-1} (\text{moles/l})^{-0.5}$$

For test n. 2, in the same way, we get $E/R = 9040^\circ\text{K}$, $E = 18.0$ kcal/mole,

$y_r = -3.594$, $x_0 = 9.59$ moles/l, $K_r = 11.1 \cdot 10^{-2} \text{min}^{-1} (\text{moles/l})^{-0.5}$.

In table 3 we report starting data and essential results of the two tests.

Table 3

Test n.	x_0, form (moles/l)	x_0, phenol (moles/l)	x_{NaOH} (moles/l)	ΔH (kcal/mole)	E (kcal/mole)	n	K_r (at 100°C) $\text{min}^{-1}(\text{moles/l})^{-0.5}$
1	9.88	4.78	0.112	13.7	17.4	1.5	$2.95 \cdot 10^{-2}$
2	9.59	4.64	0.350	13.7	18.0	1.5	$11.1 \cdot 10^{-2}$

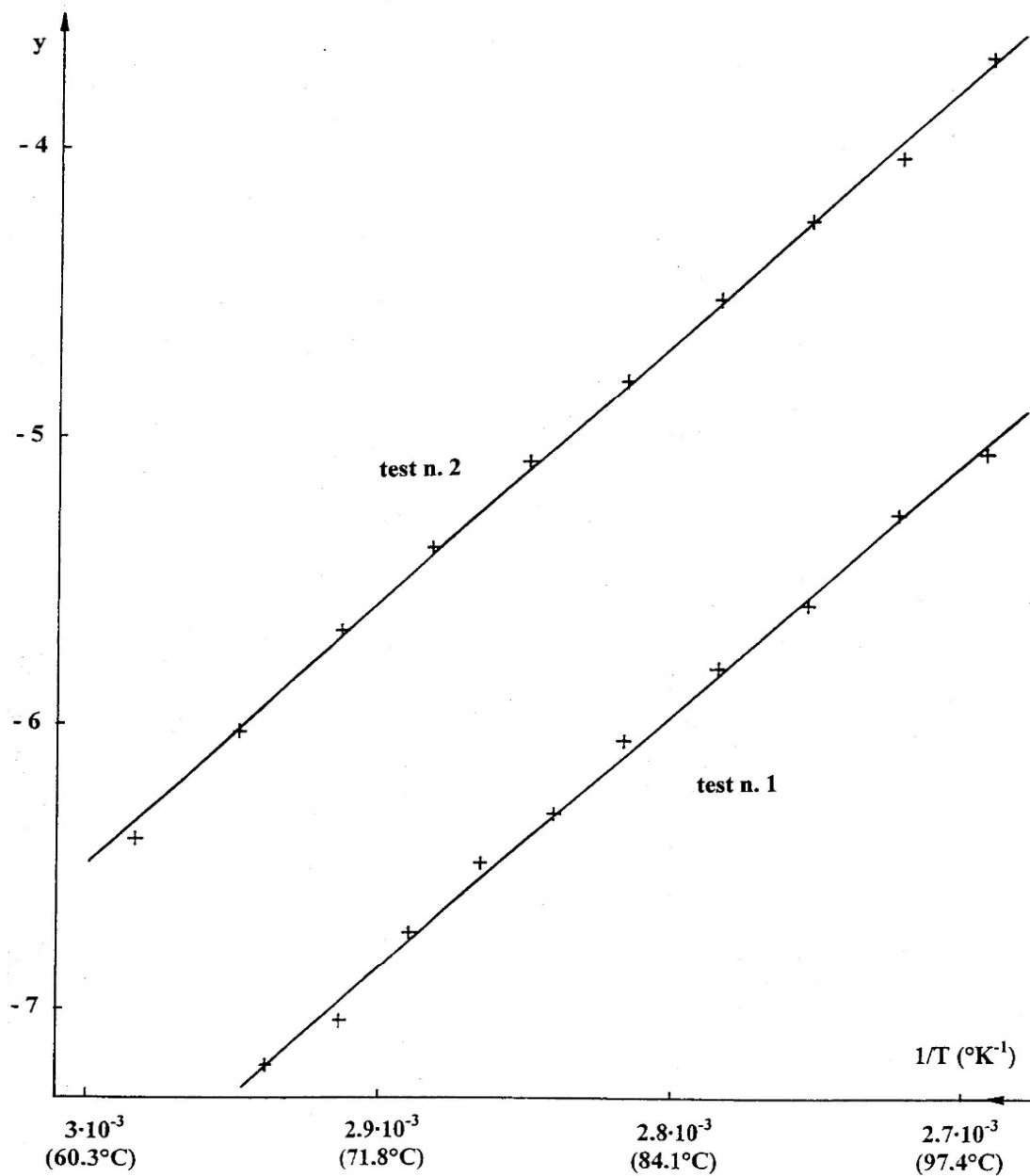


Fig. 11 - Interpolating plots of $y = \ln \left[\frac{dT/dt}{(T_F - T)^{1.5}} \right]$ versus $1/T$

Catalyst concentration x_{NaOH} is the only substantial change in the two tests. The ratio between phenol concentrations, almost unit, is the same as for formaldehyde. The slight difference is due to the larger quantity of 30% caustic soda added in the second test; with the same overall weight (5 kg) and the same volume of reactive mixture, phenol and formaldehyde concentrations turn out obviously to be slightly lower.

Comparing the two K_r , we deduce that the reaction rate is proportional to $x_{\text{NaOH}}^{1.16}$, that is little more than directly proportional to that parameter (at least in the explored concentration range). In effect this type of dependence looks plausible, taking into account what we said in par. 1.2. The experimental confirmation is however very remarkable, if we consider that other sources give quite contradictory information on this matter.

The report by British Plastics Federation [8] mentions in the text rate rises by 2.4 times for a doubling of catalyst concentration (which means an exponent 1.26 for x_{NaOH}), but it shows some plots in which the rise is by over 5 times (exponent 2.4).

Leung and Fauske [16] mention an astonishing rise by 10 times in heat production consequent to a doubling of caustic soda quantity.

One can deduce from the above that it is always convenient, in order to obtain the rate constant, to perform specific experimental tests using the particular recipe in question, also because it is quite plausible that the molar ratio between formaldehyde and phenol as well has a remarkable influence in this regard (a matter not faced here).

Coming back to our calculations, to find the values of dT/dt relevant to an industrial reactor and necessary for rupture disk sizing it is sufficient to apply (1.8) after calculating the new values (for $\phi = 1$) of ΔT_{ad} and T_f .

With reference to the recipe of test n. 1, the value of ΔT_{ad} valid for an industrial reactor is the one previously calculated for the pilot reactor, simply multiplied by $\phi = 1.1$.

Therefore we have $\Delta T_{ad} = 160 \cdot 1.1 = 176^\circ\text{K}$.

Supposing that the mass, with the whole catalyst load, begins to react at $T_0 = 60^\circ\text{C}$ (333°K) in adiabatic conditions (without cooling), we can calculate which is the temperature rising rate when the set pressure of the rupture disk (assumed equal to 1.7 bara, corresponding to 388°K) is reached. We have $T_f = 333 + 176 = 509^\circ\text{K}$ and

$$\frac{dT}{dt} = 2.95 \cdot 10^{-2} \cdot \exp \left[\frac{17.4 \cdot 10^3}{1.987} \left(\frac{1}{373} - \frac{1}{388} \right) \right] \cdot \sqrt{\frac{9.88}{176}} \cdot (509 - 388)^{1.5} = 23.1^\circ\text{K}/\text{min}$$

3.2. MEASUREMENTS ON INDUSTRIAL REACTOR

Some industrial phenolic reactors are operated in such a way that it is possible to get directly the data necessary for our purposes, without strictly the need of testing with a pilot apparatus.

We mention for instance a case in which the reactive mixture is heated up to 65°C with steam in the jacket; then it is left to self-heating (in practically adiabatic conditions) up to about 80°C; at last it is cooled by water (through jacket and inner coil) to slow down the temperature rise up to 100°C, when boiling begins (under the control of a reflux condenser).

The period of adiabatic self-heating, about 15' long, is particularly interesting, because it represents in practice the starting phase of a hypothetical phenomenon of loss of control of the reaction.

Recorded values of temperature against time during that period obey the expressions obtained in par. 1.1.1, and from them we can get therefore easily enough the thermokinetic parameters necessary to extrapolate the trend of those 15 minutes to the following period, in the accidental hypothesis that, contrary to what normally happens, it should be impossible to cool down the reacting mass through the available devices of thermal exchange.

In particular we got from the recorded graph the values of the slopes (dT/dt) for $T = 66^\circ\text{C}$ (i.e. about 1.5' after steam cut off, in order to remove spurious transient influences) and for $T = 81^\circ\text{C}$ (i.e. in the moment of opening of cooling water inlet valve).

In our case we got dT/dt values equal respectively to 0.70 and 1.80 °C/min.

If we know ΔH and n from another source, the two couples of values of dT/dt and T allow the calculation of K_r and E .

This method is however less accurate than the one shown in par. 3.1, because the available points are only two and the temperature interval is smaller (and farther from the temperature range corresponding to usual set points of rupture disks).

On the other hand we already saw that, for our purposes, it is not necessary to know n exactly (we can easily assume here too $n = 1.5$).

As for ΔH , the remarks made towards the end of par. 1.2.1 (see expression 1.10) suggest to take a value of 11 kcal/mole, valid in the most usual range of values (1.7÷2) of molar ratio R .

Tests described in par. 3.1 steer towards higher values (14 kcal/mole, conservatively). We will perform the following calculations using alternatively both values, because we deem it suitable and instructive to evaluate the influence of such a difference in so important a parameter as ΔH on the final result (i.e. on the rupture disk diameter).

So we will be able to check what we said towards the end of par. 1.2.2, that is that the fact of “forcing” the whole set of chosen parameters to satisfy the path of the available share of the experimental curve of temperature rise makes modest the final error consequent to an even remarkable inaccuracy in one of the parameters (provided the others are fixed consistently).

We point out that the aforesaid check is, in this case, even more meaningful than the one applicable to the results of par. 3.1, because the experimental temperature interval (65÷81°C) is much farther from the range of interest for disk sizing (115÷130°C).

Coming to the evaluation of E and K_r , we notice that the problem of ϕ , in this case, does not hold, because experimental data come directly from the industrial reactor (in the various relevant formulas we may consider therefore $\phi = 1$).

As from (1.6), we have $T_f = T_0 + \Delta T_{ad}$, where (with $\phi = 1$)

$$\Delta T_{ad} = \frac{\Delta H \cdot V_l \cdot x_0}{M \cdot C_p} = \frac{\Delta H \cdot x_0}{\rho_l \cdot C_p}$$

In the 18 m³ reactor 15,000 kg of reactive mixture are loaded, with density $\rho_l = 1.1$ kg/l and initial formaldehyde concentration equal to 9.5 moles/l.

Considering $\Delta H = 11$ kcal/mole we get $\Delta T_{ad} = 11 \cdot 9.5 / 1.1 / 0.7 = 135.7^\circ\text{C}$ and $T_f = 65 + 135.7 = 200.7^\circ\text{C}$.

In the two points (1 and 2) in which we measured the slope dT/dt of the recorded curve we have therefore:

$$\frac{1}{T_1} = \frac{1}{(66 + 273)} = 2.950 \cdot 10^{-3} \text{ } ^\circ\text{K}^{-1}$$

$$y_1 = \ln \frac{dT/dt}{(T_f - T_1)^n} = \ln \frac{0.70}{(200.7 - 66)^{1.5}} = -7.711$$

$$\frac{1}{T_2} = \frac{1}{(81 + 273)} = 2.825 \cdot 10^{-3} \text{ } ^\circ\text{K}^{-1} \quad y_2 = \ln \frac{1.80}{(200.7 - 81)^{1.5}} = -6.590$$

The slope of the straight line joining the two points $(1/T_1; y_1)$ and $(1/T_2; y_2)$ is worth $-E/R$ and is given by $(y_2 - y_1)/\left(\frac{1}{T_2} - \frac{1}{T_1}\right) = -8973$, therefore $E = 8973 \cdot 1.987 \cdot 10^{-3} = 17.8 \text{ kcal/mole}$.

The ordinate y_r of the line, in correspondence of $1/T = 1/T_r$ (we assume $T_r = 373 \text{ } ^\circ\text{K}$, i.e. 100°C , as the reference temperature), gives the value of K_r .

More exactly we have, taking into account the expression (1.8)

$$K_r \cdot \sqrt{\frac{x_0}{\Delta T_{ad}}} = e^{y_r} \quad \text{from which} \quad K_r = e^{y_r} \sqrt{\frac{\Delta H}{\rho_l \cdot C_p}}$$

Being $y_r = -5.299$ we get

$$K_r = e^{-5.299} \cdot \sqrt{\frac{11}{1.1 \cdot 0.7}} = 1.89 \cdot 10^{-2} \text{ min}^{-1} (\text{moles/l})^{-0.5}$$

On the contrary if we consider $\Delta H = 14 \text{ kcal/mole}$ we get in the same way $\Delta T_{ad} = 172.7^\circ\text{C}$, $T_f = 237.7^\circ\text{C}$, $E = 17.2 \text{ kcal/mole}$, $y_r = -5.749$ and $K_r = 1.36 \cdot 10^{-2} \text{ min}^{-1} (\text{moles/l})^{-0.5}$.

Notice how, when ΔH varies, E and K_r change too to form a set of values still able to faithfully reproduce the experimental curve.

A possible check, useful to test the validity of formulated hypotheses ($n = 1.5$ and linearity of y against $1/T$ in the whole self-heating interval), is that of calculating through (1.9) the time t necessary to go from 65 to 81°C and comparing it with the experimental one (15.2'). It is necessary to solve numerically the integral

$$t = \frac{\left(\frac{\Delta T_{ad}}{x_0}\right)^{0.5}}{K_r} \cdot \int_{T_0}^{T_2} \frac{e^{\frac{E}{R}\left(\frac{1}{T} - \frac{1}{T_r}\right)}}{(T_f - T)^{1.5}} dT$$

where $(\Delta T_{ad}/x_0)^{0.5}/K_r = e^{-y_r}$, $T_0 = 338^\circ\text{K}$, $T_2 = 354^\circ\text{K}$, $T_r = 373^\circ\text{K}$.

In the first case ($\Delta H = 11 \text{ kcal/mole}$) we have $e^{-y_r} = e^{5.299}$, $E = 17.8 \text{ kcal/mole}$, $T_f = 473.7^\circ\text{K}$ and we get $t = 15.2'$. In the second case ($\Delta H = 14 \text{ kcal/mole}$) we have $e^{-y_r} = e^{5.749}$, $E = 17.2 \text{ kcal/mole}$, $T_f = 510.7^\circ\text{K}$ and we still get $t = 15.2'$.

The two results coincide between them and with the experimental value, which confirms besides that both sets of parameters correctly describe the recorded curve share.

4. RUPTURE DISK SIZING

4.1. PRELIMINARY REMARKS

We will apply the developed calculation procedures and the obtained experimental results to the evaluation of the diameter D_r of the rupture disk necessary to discharge from the reactor, with an acceptable overpressure, the reacting mixture and the generated vapours.

The accident hypothesis is the loss of reaction control (for instance for lack of cooling water or for mixer failure) immediately after the end of the initial heating with steam and the catalyst addition, with the following course of the reaction in adiabatic conditions.

The operating strategy described at the beginning of par. 3.2 is only one of those usually applied.

Other systems, more careful and modern, provide, after the starting heating with steam up to 55÷60°C, a course of the initial reaction phases at constant temperature (thanks to the automatic control of the cooling circuit), with a progressive dosing of either catalyst or formaldehyde.

Only in a second time temperature is allowed to rise (not necessarily up to 100°C) to complete the phase of condensation and resol formation.

In practice it is suitable to avoid the contemporary presence of high concentrations of formaldehyde and catalyst, already at low temperatures and even more at the high ones, otherwise there is the risk that:

- The cooling system is not able to keep the reacting mass temperature at the constant value wanted during the first stage
- in case of immediate loss of reaction control the rupture disk set point is reached with so high a temperature rising velocity as to require exorbitant vent areas.

Both dosing techniques show some problems.

Continuous dosing or stepped addition of catalyst are operations to be subjected to a strict procedure, with redundant devices that should virtually exclude all possibility of mistake (for instance loading the catalyst all in one go).

Progressive formaldehyde feeding requires to suitably relate the flow rate to the constant working temperature: if this is too low there is the risk of generating unreacted formaldehyde concentrations that recreate the typical dangers of traditional batch processes.

As already mentioned, we will analyse the failure scenario, very simple, just relevant to a traditional system in which all the catalyst is added to the whole reactive mass all in one go at the end of the heating phase (it is usually the case of recipes that involve medium-low catalyst quantities).

The expressions obtained in par. 1.1.1 allow, with simple developments, to analyse also the more complex systems involving continuous dosing or stepped addition, so as to identify the most critical moment in which to suppose the loss of reaction control (this moment will correspond to the maximum possible size for the rupture disk).

However this purely mathematical analysis must not make us disregard another type of analysis, not faced here, i.e. the identification of plausible failure scenarios (it is necessary for instance to consider the possibilities of human error in the catalyst loading procedure, in the timely interruption of the initial phase of steam heating, etc.).

It is indeed a sure thing that, however refined the performed calculations may be, their results can never be more valid than the assumed failure scenario.

4.2. CHOICE OF DISK SET PRESSURE

For disk sizing the first problem is that of fixing P_s and P_m , i.e. the corresponding temperatures T_s and T_m .

As for the maximum pressure P_m , the matter was already faced in par. 1.3.1: it is necessary in practice to calculate the disk area for various P_m values, to plot the typical knee-shaped curve and at last to choose P_m within the values corresponding to the knee of the same curve (and not much further).

The above plotting involves however to have already chosen the set pressure P_s (and therefore T_s).

In this connection it is rather intuitive that it is suitable to choose P_s slightly higher than the normal working pressure. In fact, if we let temperature rise up to a value T_s much higher than the maximum working temperature, owing to the exponential Arrhenius law the reaction rate will reach such values as to generate thermal powers requiring much larger vent areas, in spite of the beneficial effect of the higher pressure on the specific discharge flow rate G (we saw in par. 1.3.2 that G is directly proportional to P).

Another reason for not choosing too high a P_s value is that reaching the corresponding T_s , together with the following vent phase, necessarily involve a rather large formaldehyde consumption in comparison with the overall available amount. These high conversion degrees, associated with the very high temperatures reached in this case, may correspond to incipient cross-linking of the polymeric chains and to resin gelification, with remarkable increase of viscosity and consequent greater discharge difficulties, or even dangerous clogging of vent areas.

At this point it is right to wonder how much P_s should be near to working pressure P_n . If this is definitely higher than pressure P_a prevailing in the discharge environment, then it is sufficient to provide a margin between P_n and P_s to absorb the possible fluctuations of P_n and to take into account the tolerance in disk set pressure.

If on the contrary, as it often happens in the case of phenolic resins, P_n and P_a coincide in practice with atmospheric pressure, it is also necessary to consider that, in the two-phase regime, the hydrostatic head, due to the elevation difference between the highest

point of the discharge piping and the reactor outlet nozzle, is not negligible as in the case of a purely gaseous emission.

Therefore, apart from the value of disk set point, reactor pressure will rise by an amount at least corresponding to that head before discharge actually begins.

Besides it is logical to provide a certain pressure difference available for head losses in the discharge piping and in the system of emission containment and scrubbing.

According to the report of British Plastics Federation [8] too low discharge pressures should be avoided because they would generate so long evacuation times, as to involve a degree of reaction completion sufficient to cause residual mass gelification (as, more plausibly, we saw it may happen in the case of too high P_s).

In practice, in our opinion, it is suitable to fix a value of P_s between 1.5 and 2 bara (0.5÷1 bar gage). In this way, besides, it is very probable to have a discharge in the critical regime and therefore to satisfy the hypotheses within which the formulas of par. 1.3.2 are valid.

After these preliminary remarks and taking into account that in the following example the discharge pipe is rather long and has a certain superelevation, a pressure $P_s = 1.7$ bara turns out to be here a suitable choice.

As for the maximum expected pressure P_m , the value of 2.6 bara used in the following calculation will appear fully justified only a posteriori, on the basis of the path of the knee-shaped curve plotted later on. However we point out that maximum allowable working pressures of phenolic reactors are usually definitely higher than this value.

As confirmed by many researchers (and also in [8]), the vapour pressure of the reactive mixture can be considered equal to the water one with good approximation. (*)

We assumed here an expression like (1.20) (three constant Antoine formula, adjusted through the values supplied by steam tables for 100, 110 and 120°C):

$$\ln P = A - \frac{B}{T + C} = 11.713 - \frac{3824.5}{T - 46.14} \quad \text{or} \quad T = \frac{3824.5}{11.713 - \ln P} + 46.14 \quad (4.1)$$

with P in bara and T in °K.

Then we get for $P = P_s = 1.7$ bara $T = T_s = 388.2^\circ\text{K}$ and for $P = P_m = 2.6$ bara $T = T_m = 401.7^\circ\text{K}$.

(*) However, if more accurate data are available through a VSP test, they obviously have the prevalence.

4.3. VENT AREA CALCULATION IN TWO-PHASE FLOW CONDITIONS

We consider first the hypothesis of $\Delta H = 11$ kcal/mole.

Having conservatively supposed the loss of control immediately after the beginning of the reaction, we assume $T_0 = 65^\circ\text{C}$ as the temperature at which adiabatic rise begins.

As already in par. 3.2 it is $x_0 = 9.5$ moles/l, $\Delta T_{ad} = 135.7^\circ\text{C}$ and $T_f = T_0 + \Delta T_{ad} = 65 + 273 + 135.7 = 473.7^\circ\text{K}$.

Besides it is still $E = 17.8$ kcal/mole, $T_r = 373^\circ\text{K}$, $K_r = 1.89 \cdot 10^{-2} \text{ min}^{-1} (\text{moles/l})^{-0.5}$.

Expression (1.8) may be so rewritten (for $n = 1.5$)

$$\left(\frac{dT}{dt}\right)_p = K_r \cdot \exp\left[\frac{E}{R}\left(\frac{1}{T_r} - \frac{1}{T}\right)\right] \cdot \left(\frac{x_0}{\Delta T_{ad}}\right)^{0.5} \cdot (T_f - T)^{1.5} \quad (4.2)$$

For $T = T_s$ and $T = T_m$ it gives the values necessary for calculating the q term given by (1.17).

We get respectively:

$$\left(\frac{dT}{dt}\right)_{ps} = 10.1^\circ\text{K/min} = 0.168^\circ\text{K/sec} \quad \left(\frac{dT}{dt}\right)_{pm} = 17.0^\circ\text{K/min} = 0.283^\circ\text{K/sec}$$

$$\text{and then } q = \frac{1}{2} C_p \left[\left(\frac{dT}{dt}\right)_{ps} + \left(\frac{dT}{dt}\right)_{pm} \right] = \frac{1}{2} \cdot 2930 [0.168 + 0.283] = 661 \text{ Watt/kg}$$

being $C_p = 0.7$ kcal/kg/ $^\circ\text{C} = 2930$ Joule/kg/ $^\circ\text{C}$.

As it turns out to be $\left(\frac{dT}{dt}\right)_{pm} \leq 2 \cdot \left(\frac{dT}{dt}\right)_{ps}$, the application of the Leung method does not involve reliability problems for the results.

It is then:

$$\bar{P} = (P_s + P_m)/2 = 2.15 \text{ bara} = 215,000 \text{ N/m}^2$$

$$\bar{T} = (T_s + T_m)/2 = 394.9^\circ\text{K}$$

$$\Delta P = P_m - P_s = 0.9 \text{ bar} = 90,000 \text{ N/m}^2$$

$$\Delta T = T_m - T_s = 13.5^\circ\text{C}$$

From (1.21) and (1.22) we get then:

$$\frac{m_m}{M} = 1 / \left[1 + \frac{\sqrt{C_p \Delta T}}{\sqrt{\frac{V}{M} \bar{T} \frac{\Delta P}{\Delta T}}} \right] = 1 / \left(1 + \frac{\sqrt{2930 \cdot 13.5}}{\sqrt{\frac{18}{15,000} \cdot 394.9 \cdot \frac{90,000}{13.5}}} \right) = 0.220$$

$$t_e = \frac{M}{AG} = \left[\sqrt{\frac{V}{M} \bar{T} \frac{\Delta P}{\Delta T}} + \sqrt{C_p \Delta T} \right]^2 / q = [56.2 + 198.9]^2 / 661 = 98.5 \text{ sec}$$

$$t_m = t_e \left(1 - \frac{m_m}{M} \right) = 76.8 \text{ sec}$$

$$\frac{\bar{m}}{M} = \frac{1}{2} \cdot \left(1 + \frac{m_m}{M} \right) = 0.610$$

That means that the reactor empties in 98.5 sec and reaches the maximum pressure 76.8 sec after disk burst (when the contained mass has dropped to 22% of the starting one).

Then we have from (1.27):

$$\begin{aligned} \bar{\omega} &= \left(1 - \frac{\bar{m}}{M} \cdot \frac{M}{V \rho_l} \right) \left(1 - 2 \frac{\bar{P} \Delta T}{\bar{T} \Delta P} \right) + \frac{\bar{m}}{M} \cdot \frac{M}{V} C_p \frac{\bar{P}}{\bar{T}} \left(\frac{\Delta T}{\Delta P} \right)^2 = \\ &= \left(1 - 0.610 \cdot \frac{15,000}{18 \cdot 1100} \right) \left(1 - 2 \cdot \frac{215,000}{394.9} \cdot \frac{13.5}{90,000} \right) + 0.610 \cdot \frac{15,000}{18} \cdot 2930 \cdot \frac{215,000}{394.9} \cdot \left(\frac{13.5}{90,000} \right)^2 = \\ &= 0.45 + 18.25 = 18.7 \end{aligned}$$

being $\rho_l = 1100 \text{ kg/m}^3$ the liquid density.

The reduction coefficient C_c , to be applied to $\bar{\eta}_{oc}$ and to \bar{G}_{oc} to take into account the conveying pipe for emergency discharge, depends, besides on $\bar{\omega}$, also on N_t (number of velocity heads corresponding to pressure losses) and on $\bar{F}l$ (modified Froude number, which includes the elevation H of pipe outlet with reference to reactor outlet nozzle).

The pipe, about 24 m long (L), includes: a square cut entrance ($N = 0.5$), three long-radius 90° elbows ($R/D = 1.5$ and therefore $N = 0.25 \cdot 3$) and a rupture disk (of the type with one-side support against vacuum).

The diameter D of pipe and disk is still unknown and therefore, to calculate L/D and then friction losses along the pipe, it is necessary to fix here a value for D and to go on by trial and error.

Assuming $D = 0.4 \text{ m}$, we have $L/D = 60$, which must be divided by 50 (as seen in par. 1.3.2) to get N .

For pipe friction losses we have therefore $N = 1.2$.

As for the disk, the type in question, when broken, gives a contribution of about $N = 0.3$ if its diameter is exactly equal to the pipe one. (*)

The overall value $N_t = \sum N$, due to the contribution of the various resistances, is therefore equal to $1.2 + 3 \cdot 0.25 + 0.5 + 0.3 = 2.75$.

Elevation H is worth about 2 m in our configuration (therefore H and Fi are positive).

Then we have from (1.33):

$$\bar{F}i = \frac{\bar{m}}{M} \cdot \frac{M}{V} \cdot \frac{gH}{N_t \bar{P}} = 0.610 \cdot \frac{15,000}{18} \cdot \frac{9.81 \cdot 2}{2.75 \cdot 215,000} = 0.0169$$

From the expression (A.7) of Appendix I we get (for $\bar{\omega} = 18.7$, $\bar{F}i = 0.0169$ and $N_t = 2.75$) $a = 0.1869$, $b = 0.7447$ and at last $C_c = 1/(1 + aN_t^b) = 0.7158$.

Being $10 \leq \bar{\omega} \leq 40$, $0 \leq \bar{F}i \leq 0.05$ and $C_c \geq 0.6$, this result is certainly a good approximation of the rigorous one (which in fact is worth 0.71565).

The effective critical ratio $\bar{\eta}_c$ is then equal to, for (1.34) and (1.29):

$$\bar{\eta}_c = C_c \cdot (0.6055 + 0.1356 \ln \bar{\omega} - 0.0131 \ln^2 \bar{\omega}) = 0.716 \cdot 0.890 = 0.637$$

Therefore we have, for (1.31) and (1.32):

$$\bar{G} = \frac{\bar{\eta}_c}{\sqrt{\bar{\omega}}} \cdot \sqrt{\bar{P} \cdot \frac{\bar{m}}{M} \cdot \frac{M}{V}} = \frac{0.637}{\sqrt{18.7}} \cdot \sqrt{215,000 \cdot 0.610 \cdot \frac{15,000}{18}} = 1540 \text{ kg/sec/m}^2$$

At last, from (1.16) or faster from the expression of $t_e = M/(\bar{G}A)$, we get

$$A = \frac{M}{\bar{G}t_e} = \frac{15,000}{1540 \cdot 98.5} = 0,0989 \text{ m}^2$$

This value must be divided by 0.9 according to ASME provisions (1997 Addendum), to take account of the uncertainties of the method using K_R and N_t .

We get $A_d = A / 0.9 = 0.110 \text{ m}^2$ which means a disk of diameter $D_r = 374 \text{ mm}$.

The obtained value is close enough to the one assumed for N_t calculation to make a possible iteration practically unimportant for the final result (as one can easily check).

(*) This N should be exactly equal to the certified flow resistance factor K_R for the rupture disk device.

If, for disk support problems, it should be suitable to choose a disk diameter slightly smaller than the pipe one, then the resistance of disk residual parts would add to the resistance of the supporting ring projecting towards the pipe centre. This resistance corresponds to about $N = 0.6$ in the case that the ratio between the two diameters is 0.9 (very interesting experimental results referring to such a diaphragm and to various disk types are reported in [19]). So, in this case, overall disk contribution is $N = 0.9$.

As the burst disk (including the possible supporting ring) is dealt with exactly as any fitting along the pipe, the vent area obtained through (1.16) represents the duct section, and not the disk one.

The pressure P_a in the container into which emission is discharged is equal to the atmospheric one plus the back pressure generated by the possible following emergency scrubber.

If this is a condensing tower, with direct contact of the effluent with a washing liquid, back pressure is practically negligible ($P_a = 1$ bara).

If on the contrary one chooses a passive quench pool (i.e. a vessel containing a suitable water volume, into which the vapours are dispersed and condensed), back pressure depends on the provided hydrostatic head (which in our case could be of about 0.8 m; therefore $P_a = 1.08$ bara).

It is then necessary to check that P_a/P_s is smaller than $\bar{\eta}_c$, i.e. that the hypothesis of critical conditions is actually satisfied (otherwise the flow \bar{G} would be smaller than supposed and would be however given by formulas different from the used ones).

As $P_a/P_s = 1.08/1.7 = 0.635 < 0.637$, the condition is satisfied.

Even if here $\omega \neq 1$ and $Fi \neq 0$, the plot of flow rate against downstream pressure remains however qualitatively similar to the one of fig. 12 in Appendix I. Therefore, even if P_a/P_s turns out to be slightly greater than $\bar{\eta}_c$, it is possible to keep still valid with no problem the value of \bar{G} calculated in the hypothesis of critical conditions.

If, leaving unchanged all the other design parameters, we let P_m vary and we plot the A values so obtained, we get the curve of fig. 9 (see par. 1.3.1), from which it is clear, on the basis of the remarks in the aforesaid paragraph, that the suitable P_m values are those in the range between 2.5 and 3.0 bara. (*)

The flat line at the base of the diagram is the one obtained in the (unrealistic) hypothesis of all-vapour venting (consequent to a perfect disengagement of liquid and gaseous phases).

(*) It is interesting to note that, for $P_m = 2.6$ bara, if instead of the arithmetic mean between $(dT/dt)_{ps}$ and $(dT/dt)_{pm}$ we had taken the more rational integral mean described in Appendix III, we would have obtained a value for $q = 676$ W/kg (only 2% higher). Geometric and logarithmic means lead to much lower values (and therefore unreliable). But even more interesting is the fact that, for instance for $P_m = 4$ bara (and therefore with a remarkable overpressure and with a ratio $(dT/dt)_{pm} / (dT/dt)_{ps} = 2.64$, much greater than 2), the q value given by the integral mean is still only 2% higher than that obtained with the arithmetic mean, which therefore remains, in its simplicity, a working hypothesis entirely valid.

Relevant calculations are reported in the following paragraph.

If we assume $\Delta H = 14$ (instead of 11) kcal/mole (and therefore $E = 17.2$ kcal/mole and $K_r = 1.36 \cdot 10^{-2} \text{ min}^{-1} (\text{moles/l})^{-0.5}$), we obtain, in short, the following different results:

$$\Delta T_{ad} = 172.7^\circ\text{C}; \quad T_f = 510.7^\circ\text{K};$$

$$\left(\frac{dT}{dt}\right)_{ps} = 10.7^\circ\text{K/min}; \quad \left(\frac{dT}{dt}\right)_{pm} = 19.0^\circ\text{K/min}; \quad q = 726 \text{ Watt/kg};$$

$$t_e = 89.7 \text{ sec}; \quad t_m = 69.9 \text{ sec}; \quad A = 0.109 \text{ m}^2; \quad A_d = 0.121 \text{ m}^2 \quad (D_r = 393 \text{ mm}).$$

But there is no change in the values of parameters $\frac{m_m}{M}, \bar{m}, \bar{\omega}, \bar{F}l, N_t, C_c, \bar{\eta}_c, \bar{G}$.

The rupture disk diameter turns out to be therefore only slightly larger than the value (374 mm) previously obtained for $\Delta H = 11$ kcal/mole, which confirms what often repeated about the poor influence of the possible uncertainty with which one knows a single thermokinetic parameter, provided the set of the values of $\Delta H, K$ and E is congruent with a large enough experimental part of the curve of adiabatic temperature rise.

To conclude, it is logical to assume a value of 400 mm as the diameter of the rupture disk and of the vent piping, with a small margin of safety in order to take into account also possible recipes and/or scenarios slightly more critical than those relevant to the performed example.

This choice means in practice that, with the recipe and the scenario above considered, maximum pressure P_m will be indeed equal not to 2.6 bara, but to 2.31 bara (as we can see from fig. 9 for $A = 0.126 \text{ m}^2$, corresponding to a 400 mm diameter pipe).

As for the thrust on such a pipe, dynamic effects included, it turns out to be equal, on the basis of the remarks of par. 1.3.3, to

$$T = 2 \cdot (P_m - P_a) \cdot A = 2 \cdot (2.6 - 1) \cdot 10^5 \cdot 0.126 = 40,300 \text{ N} = 4,100 \text{ kg}$$

Conservatively we assumed $P_a = 1$ bara, disregarding the possible back pressure due to the scrubbing system, and we kept the value $P_m = 2.6$ bara associating it to $A = 0.126 \text{ m}^2$. It is interesting at last to evaluate the elapsed time t_s between the loss of reaction control and the disk burst, so as to have an idea of the available margin for possible emergency interventions.

It may be obtained from (1.9), so rewritten:

$$t_s = \frac{\left(\frac{\Delta T_{ad}}{x_0}\right)^{0.5}}{K_r} \cdot \int_{T_0}^{T_s} \frac{e^{\frac{E}{R}\left(\frac{1}{T} - \frac{1}{T_r}\right)}}{(T_f - T)^{1.5}} dT$$

Solving numerically the integral in the two above examined cases, we get $t_s = 23.8'$ for $\Delta H = 11$ kcal/mole and $t_s = 23.7'$ for $\Delta H = 14$ kcal/mole.

4.4. ALL VAPOUR EMISSION

We will make the calculations relevant to the unlikely all-vapour emission for two reasons.

The first is to point out the deep difference with the above obtained values for two-phase conditions: such difference explains why rupture disks calculated in the past supposing all-vapour venting turned out to be in practice undersized and led to recurrent reactor explosions.

The second reason is that these calculations will be useful for some following remarks regarding containment systems.

Considering the flat line at the base of fig. 9, the most interesting value is the one (A_0) for $P_m = P_s$, given by formula (1.23).

To calculate the G value appearing in it we can resort either to the classic Lapple and Levenspiel charts [17; 18], or to the Leung “ ω ” method (applicable, as already said, to all-vapour emissions too).

In this last case the expression (1.25) must be so modified:

$$\omega = \left(1 - 2P \frac{v_g - v_l}{\lambda}\right) + \frac{C_p T P}{v_g} \left(\frac{v_g - v_l}{\lambda}\right)^2$$

As already seen in par. 1.3.1, using Clapeyron relation and Antoine formula we get (1.19 and 1.20a):

$$\frac{\lambda}{v_g - v_l} = \frac{BTP}{(T + C)^2}$$

Besides from saturated steam tables we obtain, for $P = 1.7$ bara, $v_g = 1.03$ m³/kg.

Therefore, for $P = P_s = 1.7$ bara and $T = T_s = 388.2^\circ\text{K}$, we get, taking into account the coefficients of (4.1):

$$\frac{\lambda}{v_g - v_l} = \frac{3824.5 \cdot 388.2 \cdot 1.7 \cdot 10^5}{(388.2 - 46.14)^2} = 2.157 \cdot 10^6 \text{ Joule/m}^3$$

$$\omega = \left(1 - 2 \cdot \frac{1.7 \cdot 10^5}{2.157 \cdot 10^6}\right) + \frac{2930 \cdot 388.2 \cdot 1.7 \cdot 10^5}{1.03} \cdot \frac{1}{(2.157 \cdot 10^6)^2} = 0.8424 + 0.0403 = 0.883$$

From the expression (1.29), valid for frictionless nozzles, we get, for this ω value, $\eta_{oc} = 0.5884$ (the rigorous result given by (A.5) in Appendix I is 0.5903).

Owing to (1.30) we have

$$\frac{G_{oc}}{\sqrt{P/v_g}} = \frac{\eta_{oc}}{\sqrt{\omega}}$$

from which we get

$$G_{oc} = \sqrt{\frac{1.7 \cdot 10^5}{1.03} \cdot \frac{0.59}{\sqrt{0.883}}} = 255 \text{ kg/sec/m}^2$$

To this value we must apply two corrective coefficients: C_c and C_F .

Assuming a disk and pipe diameter of about 200 mm, for the purpose of C_c calculation we get $N_t = 3.95$ instead of the previous value 2.75.

From (A.8) of Appendix I, for $\omega = 0.883$ and $N_t = 3.95$, we get $a = 0,4948$, $b = 0,8294$ and $C_c = [1 / (1 + aN_t^b)]^{0.58} = 0.582$.

The second coefficient (C_F) is due to the fact that, in the case of pure vapour, venting no longer occurs, actually, in critical conditions.

In fact critical ratio η_c is worth now (for 1.34) $\eta_c = C_c \cdot \eta_{oc} = 0.582 \cdot 0.59 = 0.343$.

Being $\eta = P_a/P_s = 0.635 > 0.343$, the condition for critical regime is no longer satisfied.

The corrective coefficient C_F , which allows to take account of that, is obtained from (A.9) in Appendix I.

In our case $(\eta - \eta_c)/(1 - \eta_c) = (0.635 - 0.343) / (1 - 0.343) = 0.444$ and therefore $C_F = \sqrt{1 - 0.444^2} = 0.896$.

At last

$$G = G_{oc} \cdot C_c \cdot C_F = 255 \cdot 0.582 \cdot 0.896 = 133 \text{ kg/sec/m}^2$$

With the Lapple-Levenspiel method we first calculate the flow through a frictionless nozzle

$$G^* = \sqrt{\frac{P_s}{v_g} \cdot k \left(\frac{2}{k+1}\right)^{\frac{k+1}{k-1}}} = \sqrt{\frac{1.7 \cdot 10^5}{1.03} \cdot 1.135 \left(\frac{2}{1.135+1}\right)^{\frac{1.135+1}{1.135-1}}} = 258 \text{ kg/sec/m}^2$$

where k is worth 1.135 for saturated steam.

From the proper chart we then evaluate, for $N_t = 3.95$ and $\eta = P_a/P_s = 0.635$, the coefficient G/G^* , which turns out to be 0.508. (*)

Therefore we have $G = 258 \cdot 0.508 = 131 \text{ kg/sec/m}^2$, a result very close to the one obtained with “ ω ” method.

We get at last (1.23)

$$A_0 = \frac{Mq}{Gv_g} \cdot \frac{v_g - v_l}{\lambda} = \frac{MC_p \left(\frac{dT}{dt}\right)_{ps}}{Gv_g} \cdot \frac{v_g - v_l}{\lambda} = \frac{15,000 \cdot 2930 \cdot 0.168}{133 \cdot 1.03} \cdot \frac{1}{2.157 \cdot 10^6} = 0.0250 \text{ m}^2$$

Applying the safety factor 0.9 provided by ASME we get $A_d = A_0/0.9 = 0.0278 \text{ m}^2$, corresponding to $D_r = 188 \text{ mm}$.

We used here the value of $\left(\frac{dT}{dt}\right)_{ps}$ valid in the hypothesis of $\Delta H = 11 \text{ kcal/mole}$.

Considering $\Delta H = 14 \text{ kcal/mole}$ and therefore $\left(\frac{dT}{dt}\right)_{ps} = 0.178^\circ\text{K/sec}$, we get correspondingly $A_0 = 0.0265 \text{ m}^2$, $A_d = 0.0294 \text{ m}^2$ and $D_r = 194 \text{ mm}$.

The disk area turns out to be therefore about 4 times smaller than the one obtained in the hypothesis of two-phase flow conditions.

The obtained diameters are close enough to the one supposed for N_t calculation to exclude the need of iterations.

- (*) This value was actually calculated through the equations that originate the plotted curves, which do not allow easy interpolations. Besides there is an inversion, both in the original Levenspiel's work and in literature reprints (for instance in ed. VI and following of Perry's Chemical Engineers' Handbook), between the values of k (1.2 and 1.6) to couple with the respective curves marked by G/G^* parameter. The fact was reported to Mr. Levenspiel in 2008.

5. EMISSION CONTAINMENT

Even if the frequency of occurrence of an emergency discharge is very low, nowadays an uncontrolled emission into the atmosphere is usually no longer allowed.

Containment systems described in literature [14] are various, depending also on the nature of the emission.

It is particularly important if it is made up also by solid or liquid state material and if vapours are completely condensable or not.

The presence of liquid matter is implied by the hypothesis of two-phase flow and must be practically and regularly taken into account in emergency discharge from reactors.

Actually some device for containment and separation of entrained liquid is usually present downstream every chemical reactor.

The minimum provision is a “dump tank” into which the emission is discharged so as to impact against a wall. The collision in itself tends to separate the liquid, which has a greater inertia than the gas, so that the former settles on the bottom of the vessel and the latter deviates towards some exhaust nozzle.

Such vessels are usually $1.5 \div 2$ times as big as the reactor.

Other systems, a bit more sophisticated, provide for a tangential inlet into the vessel, shaped as a big cyclone whose bottom acts as a reservoir. Otherwise near the reactor a real separating cyclone is placed, whose bottom discharge carries the liquid in a proper tank.

While the presence of such devices is quite frequent, much rarer is the case in which some treatment is provided for the residual gaseous stream.

If this is mainly noncondensable, it is necessary to set up a scrubber quite similar to the ones used by industry for process gas purification (for instance a baffle-spray tower rather than a packing tower, to avoid plugging problems).

If the gaseous stream is essentially made up by condensable vapours, as in our case, then, besides a scrubber, it is possible to use a passive quench tank, which actually offers numerous advantages.

Such a tank contains a suitable water volume, which cools down and condenses the vapours dispersed into the liquid through a proper sparger.

The “passive” attribute comes from the fact that the energy for dispersion and heat and mass transfer between liquid and vapours is supplied by the gas itself.

The necessary tank (usually 2÷3 times the reactor volume) is not much greater than a classic “dump tank”, and takes even its place (unlike a scrubber, which needs anyway an upstream container for the liquid phase).

Besides a quench tank is quite simpler and less expensive than a scrubber.

But perhaps the most valuable feature is that its sizing only depends on the total heat amount to be removed, and not also on the thermal power, i.e. on the instantaneous discharge flow (as it happens on the contrary with scrubbers).

To fully understand this advantage it is necessary to do some preliminary quantitative evaluations about the size and the composition of the discharge flow.

In par. 4.3 we calculated that, in the average emission conditions ($\bar{P} = 2.15$ bara), we have:

$$\bar{\omega} = 18,7 \quad \frac{\bar{m}}{M} = 0,610 \quad \text{and} \quad \bar{G} = 1540 \text{ kg/sec/m}^2$$

From the equation of state (1.24) it is possible to calculate the specific volume v of the two-phase mixture at the exhaust pipe outlet, where pressure is $P_a = 1.08$ bara, knowing the conditions at the inlet of the same pipe:

$$\left(P_0 = \bar{P} = 2.15 \text{ bara}; v_0 = \frac{V}{\bar{m}} = \frac{V}{M} / \frac{M}{\bar{m}} = \frac{18}{15,000} / 0.610 = 1.967 \cdot 10^{-3} \text{ m}^3/\text{kg} \right)$$

We get

$$\frac{v}{1.967 \cdot 10^{-3}} - 1 = 18.7 \left(\frac{2.15}{1.08} - 1 \right) \quad v = 3.84 \cdot 10^{-2} \text{ m}^3/\text{kg}$$

As we have also $v = v_l + x(v_g - v_l)$, where x is the vapour title (i.e. its weight fraction in the mixture), we can obtain

$$x = \frac{v - v_l}{v_g - v_l} = \frac{3.84 \cdot 10^{-2} - 1/1100}{1.57 - 1/1100} = 0.024$$

being 1100 kg/m³ the liquid density and 1.57 m³/kg the specific volume of saturated steam at 1.08 bara.

As we chose a rupture disk with 400 mm diameter, the discharge area is 0.126 m².

Multiplying it by the specific flow $\bar{G} = 1540$ kg/sec/m², we get a value of 194 kg/sec for the two-phase effluent, made up for 2.4% (4.7 kg/sec) by vapour and for the rest by liquid.

If we do a similar calculation with reference to the initial condition ($P_0 = P_s = 1.7$ bara) and to the one of maximum pressure in the reactor ($P_0 = P_m = 2.6$ bara), we get vapour flows respectively equal to 2.6 kg/sec and 6.9 kg/sec (while total two-phase flow remains essentially unchanged).

We remind that time elapsed between the two aforesaid conditions is equal to 76.8 sec.

As we already pointed out in the previous paragraphs, the hypothesis of emission of a two-phase flow, rather than pure vapour, certainly involves a bigger size for the rupture disk. However, once the disk diameter has been fixed so as to face a two-phase discharge, a pure vapour emission cannot be actually ruled out a priori.

Such a mechanism would certainly develop in conditions of full safety from the point of view of pressure rise: a review of fig. 9 suggests that, as the provided relief area is quite larger than the value (0.0278 m²) necessary to avoid overpressures, we actually have an immediately decreasing trend of pressure with time.

But the vapour flow that is generated is enormous, even if quite shorter (20÷30 sec) than the relief time that is necessary in the two-phase regime.

Therefore discharge conditions turn out to be much more severe for the emission containment system.

In particular, according to the calculations of par. 4.4, we have a value of the initial specific flow (for $T = T_s = 115.2^\circ\text{C}$) equal to 133 kg/sec/m². Moreover, taking into account that the pipe has now a bigger diameter (400 mm) in comparison with the one then assumed (200 mm), we have higher values of C_C and C_F and therefore of G (exactly 149 instead of 133 kg/sec/m²). With a relief area of 0.126 m², such a value for G implies a pure vapour flow of 18.8 kg/sec (about 4 times higher than the one emitted in two-phase regime).

It is possible to calculate that reactor temperature, at the beginning of relief, drops at a speed of about 0.8°C/sec (with a corresponding pressure decrease).

A vapour flow of 18.8 kg/sec corresponds to a thermal load, for a condensation system, of about $37 \cdot 10^6$ kcal/h.

Any scrubbing tower would require a recirculating liquid flow of about 530 m³/h to absorb such thermal load without reaching the boiling point: the size of pumps, recirculating lines and of the tower itself would be actually impracticable.

Therefore the solution of a scrubbing column can be taken into consideration, in our opinion, only if a second rupture disk is installed, in parallel to the first and with a slightly lower set pressure (for instance 1.5 bara), sized for a possible effluent made up only by vapour (the diameter turns out to be about 190 mm). The initial vapour flow is then equal to about 3.0 kg/sec and therefore of the same order of the one discharged by the bigger disk in the case of two-phase regime.

The most logical and feasible solution is however the use of passive quenching, which has no limitation in terms of instantaneous load, owing to the fact, experimentally checked, that the complete condensation of steam, injected (either pure or within a two-phase mixture) into a liquid mass through a pipe or a hole with diameter D , takes place within a distance from the same hole smaller than $1.5 \cdot D$.

It is sufficient that the cooling liquid (water in our case) remains at temperatures at least 10°C lower than the one of steam condensation (i.e. that it does not exceed 90°C).

Special precautions must however be taken in sizing the sparger, through which the two-phase mixture is dispersed into the liquid.

For instance:

- the holes must be neither too small (to avoid plugging risks), nor too big (to avoid water hammer due to the sudden abatement of the volume of steam bubbles)
- hole orientation and distribution must assure a good mixing of the whole liquid mass and the compensation of thrusts generated by water hammer (in this connection even the sparger shape must respect suitable symmetries)
- hole total area must be neither too small (not to be a controlling resistance within the discharge system made up by disk and pipe), nor too big (to assure a uniform flow through all the holes, even the farthest).

In case of application to a system that presents plugging risks we can for instance use holes with 50 mm diameter, with a spacing of $2.5 \div 3$ hole diameters centre to centre and with a total area equal to at least 1.35 times ($1/0.74$) the section of the reactor relief pipe. For critical flow through holes, the discharge coefficient is actually worth about 0.74 (instead of the usual value 0.63, typical for sub-critical conditions).

In principle the tank may have or not an exhaust pipe into the atmosphere.

If this pipe is present, a small residual emission is possible, due to the ejection of the air contained in the discharge line and in the top space of the tank (more exactly in the volume

which comes out to be occupied owing to the liquid expelled from the reactor): this air will be actually saturated with formaldehyde.

The global emission is however quite negligible (less than one hundred thousandth of the initial charge of formaldehyde in the reactor).

If the exhaust pipe is not present, any emission is avoided, but pressure in the tank grows up remarkably, especially owing to the compression of the air (present at the top of the tank) caused by the expelled reacting mass.

This involves the construction of a pressure vessel for containment (with its own rupture disk, besides) and the raising of the set value of the reactor disk.

In our case it is not certainly worthwhile turning to the closed model.

Let us come at last to the calculation of the necessary water amount and of the tank volume.

Conservatively it is convenient to imagine a complete transfer of the reactor liquid and a completion of the reaction in the quenching tank. Both things are unlikely (the second because the strong dilution with water and the temperature decrease practically block the reaction), but it is not worthwhile splitting hairs.

Therefore we will assume that the whole available heat of reaction has warmed, at first during the temperature runaway and at last during the quenching process, the cooling water from the starting value of 20°C up to 80°C (a more conservative hypothesis in comparison with the previously considered 90°C) and the reacting mass from the initial 65°C up to the final 80°C (considering that it ends up mixed with water).

Taking into account the maximum assumed heat of reaction (14 kcal/mole) and considering that 129,500 moles of formaldehyde are initially present ($x_0 \cdot M / \rho_l$), the whole available heat is equal to $14 \cdot 129,500 = 1.81 \cdot 10^6$ kcal.

The aforementioned thermal balance is then:

$$1.81 \cdot 10^6 = L \cdot 1 \cdot (80 - 20) + 15,000 \cdot 0.7 \cdot (80 - 65)$$

from which we get the necessary volume of cooling water $L = 27,500$ kg (27.5 m³).

Taking into account 13.6 m³ of reacting mass to be housed and a margin of at least 10% as the difference between the total tank volume and the usable one, we arrive at a final value of 45÷50 m³.

6. PRECAUTIONS TO AVOID REACTION RUNAWAY

The rupture disk intervention must be considered the ultimate remedy to avoid reactor explosion; but obviously a series of precautions must be carried out so as normally not to go so far, even in the presence of mishaps and failures of various kind.

Apart from the fundamental requirement of an accurate staff training, to avoid as much as possible human errors and to prepare workers to face with clearness and coolness every emergency situation, we will draw up in the following an illustrative list of some precautions taken by various companies in this line of business (this matter would obviously deserve a much deeper investigation, that goes however beyond the purposes of the present work).

- 1) Limited exploitation of reactor capacity (i.e. of 65÷70% of geometric volume), with the advantage of:
 - limiting in every operating condition the heat development, which is proportional to the volume of the reacting mass
 - saving the space for quenching the reacting mass with cold water in emergency conditions (with a procedure described later on)
 - leaving the space for (even partial) vapour disengagement during the possible discharge phase through the rupture disk.
- 2) Availability of a spare installed pump for cooling water circulation in the jacket.
If there is a pipe network connected to a water tower, it is suitable to provide for a possible emergency supply from that source.
- 3) Presence of a manual by-pass valve for every automatic control valve on cooling water and besides of two cut off valves in series on the steam pipe feeding the jacket (to avoid possible leakages in the phase in which cooling water is running through the same jacket).
- 4) Arrangement of several probes to measure reacting mass temperature (better if they are directly dipped resistance thermometers), so as, if one fails, it is possible to rely upon the others to complete the reaction.
- 5) Presence of a generator set sufficient for feeding all electric equipment (in particular cooling pumps and mixers).

It is suitable to provide also a battery no break power supply to feed instrumentation even in case of very short power breaks and therefore to avoid upsets and oscillations in automatic control systems.

6) Laboratory control, before every batch, of the titre of caustic soda to be used as catalyst.

7) Reactor operation at a controlled temperature lower than 100°C, above all in the first phase of the reaction, so as:

- to limit heat development (that depends on temperature), making its removal easier and increasing the margin of control in case of signs of runaway
- to increase the time available for emergency operations in case of loss of control.

8) Temperature control through microprocessor according to a planned cycle.

This allows to measure and keep very small offsets (less than 1°C) between read and set up temperatures (which means a process under strict control, without oscillations).

Besides it is possible to put in action advance warning signals, to immediately alert the workers, in case of moderate offsets (of about 2°C).

9) Catalyst addition in several steps, or progressive input of formaldehyde, with the advantages and the problems already outlined in par. 4.1.

10) Possibility, in case of mechanical mixer failure, of injecting some compressed air (for the necessary mixing action) through a small nozzle, with screw plug, placed on the discharge pipe of the resin (a fixed connection would turn out to be probably plugged in case of need).

The necessary flow rate (about 40 Nm³/h per m² of reactor cross section) can be exactly fixed and correlated to the pressure read downstream a suitable reducer, opening its valve to such an extent as to reproduce (in the phase of final cooling of the resin after a normal reaction cycle, and therefore in conditions of full safety) the same thermal gradient (°C/min) assured by the mechanical mixer.

11) Possibility of discharging into the reactor (even in several steps) cold water from a suitable vessel, in order to quench the reaction in emergency situations.

This system is quicker than the previous one and may be adopted for instance when mixer failure happens at rather high temperatures, which leave a short time to

intervene (it is however suitable that a clear and immediate warning of shaft stop is sent out by some rotational speed sensor).

The decrease of reaction rate (and therefore of temperature rise) is immediate and remarkable, owing both to mass cooling and to reagents and catalyst dilution. It allows therefore to recover the reaction control or at least the time necessary to make calmly the compressed air connection (for lack of agitation, and below the boiling temperature, mixing of water with the reacting mass may be poor).

12) Possibility of pH correction in the reacting mass, to minimize catalytic action.

This method has limits and must be considered with great caution, because:

- in case of agitator failure it is impossible to mix effectively the additive for pH correction and therefore to allow practically its action
- it is not possible to be lavish with additive dosage because, as we saw in par. 1.2.1, this reaction is catalyzed by both bases and acids (and by these even more violently)
- the liquid mass pH changes progressively during the reaction; therefore the additive must be measured exactly as needed and not discharged in a pre-established amount (also because the trouble might have been caused by a wrong initial dosage of the catalyst).

APPENDIX I

CALCULATION OF FLOW REDUCTION COEFFICIENT

The so-called mechanical-energy balance for a fluid flowing in a pipe may be written in the following differential form:

$$v \cdot dP + d\left(\frac{u^2}{2}\right) = -\left[\frac{4f}{D} \cdot \frac{u^2}{2} dL + g \cdot dz\right] = -\left[\frac{N_t}{L_e} \frac{u^2}{2} + \frac{Hg}{L_e}\right] dL$$

where u (m/sec) is the velocity ($u = Gv$) and the other terms were already defined in par 1.3. The first addend in the square bracket takes into account the friction losses and the second the variation of potential energy (i.e. the elevation z).

In the case of simple flow from a vessel through a frictionless nozzle these two addends lose their significance and the expression reduces to:

$$v \cdot dP + d\left(\frac{u^2}{2}\right) = v \cdot dP + \frac{1}{2} d(Gv)^2 = 0$$

Notice that no hypothesis was made on the constancy of the cross section, and therefore of G (kg/sec/m²), along the nozzle (and actually such a constancy would be inconsistent with the absence of friction).

Integrating the previous differential equation we get (subscripts 0 and 1 refer to nozzle inlet and outlet respectively):

$$G_1 = \frac{1}{v_1} \left(2 \int_{P_0}^{P_1} -v dP \right)^{1/2}$$

If we suppose a relation between v and P given by the equation of state (1.24), the elementary solution of the integral is the following (with $\eta_1 = P_1/P_0$):

$$G_1^* = \frac{G_1}{\sqrt{P_0/v_0}} = \frac{\sqrt{2[(1-\omega)(1-\eta_1) - \omega \ln \eta_1]}}{\omega \left(\frac{1}{\eta_1} - 1\right) + 1} \quad (\text{A. 1})$$

In the case of a long duct with a constant cross section (with bends and other friction sources taken into account by L_e and N_t) the differential equation becomes (now G too is constant like the cross section):

$$v \cdot dP + G^2 v \cdot \frac{dv}{dP} \cdot dP + \left(N_t \cdot \frac{G^2 v^2}{2} + Hg \right) \cdot d\left(\frac{L}{L_e}\right) = 0$$

Integrating between the ends 1 and 2 of the duct (in correspondence of which L/L_e passes from 0 to 1) we get:

$$N_t \cdot \int_0^1 d\left(\frac{L}{L_e}\right) = N_t = - \int_{P_1}^{P_2} \frac{v + G^2 v \frac{dv}{dP}}{\frac{G^2 v^2}{2} + \frac{Hg}{N_t}} dP$$

Expressing again v as a function of P through (1.24) we obtain:

$$N_t = \int_{\eta_2}^{\eta_1} \frac{\eta[\omega + (1 - \omega)\eta] \cdot [1 - \omega(G^*/\eta)^2]}{\frac{G^{*2}}{2} [\omega + (1 - \omega)\eta]^2 + \eta^2 Fi} d\eta \quad (\text{A.2})$$

where

$$G^* = \frac{G}{\sqrt{P_0/v_0}} \quad Fi = \frac{Hg}{N_t P_0 v_0} \quad \eta_1 = \frac{P_1}{P_0} \quad \eta_2 = \frac{P_2}{P_0}$$

The integral can be solved elementarily [6], but the expression of the result is so complex (and however not representable in explicit form to give G^*) that it is better to use numerical techniques (such as Cavalieri – Simpson).

It is convenient to take into account that (A.1) and (A.2) hold in both subcritical and critical flow conditions.

In this last case also the condition of choked flow must be satisfied, which imposes (in the critical point c) a velocity equal to the sonic one, that is the validity of the equation:

$$G_c = \left(-\frac{dv}{dP} \right)_c^{-0.5}$$

Using the relation between v and P given by the customary equation of state, the previous expression assumes the following form:

$$G_c^* = \frac{G_c}{\sqrt{P_0/v_0}} = \frac{\eta_c}{\sqrt{\omega}} \quad (\text{A.3})$$

If the relief device were made up by a simple frictionless nozzle, then in the critical regime both (A.1) and (A.3) must hold simultaneously. As the critical section is the outlet one, (A.3) becomes:

$$G_c^* = G_{oc}^* = \frac{G_1}{\sqrt{P_0/v_0}} = \frac{\eta_1}{\sqrt{\omega}} = \frac{\eta_{oc}}{\sqrt{\omega}} \quad (\text{A. 4})$$

where subscript *oc* holds for “critical conditions in a frictionless nozzle”.

Replacing this expression in (A.1) we get the following transcendental equation that gives the critical ratio η_{oc} as a function of ω :

$$\eta_{oc}^2 + (\omega^2 - 2\omega)(1 - \eta_{oc})^2 + 2\omega^2 \ln \eta_{oc} + 2\omega^2(1 - \eta_{oc}) = 0 \quad (\text{A. 5})$$

By the way we point out that (1.29) is nothing but an explicit approximate expression for (A.5).

Having found η_{oc} , G_{oc}^* is given directly by (A.4).

If the relief device is made up, as usual, by a nozzle (with a square cut entrance) followed by a pipe of constant cross section, it may be however considered as the sequence of a nozzle with a rounded and converging cross section (i.e. frictionless) followed by a duct with the same cross section as the end of the ideal nozzle. Among the friction elements imputed to the duct (and which make up the value of N_t) there will be also the “non-ideality” of the real nozzle (whose contribution is worth 0.5).

Having identified with subscripts 0, 1 and 2 respectively the sections of nozzle inlet, nozzle outlet (i.e. pipe inlet) and of pipe outlet, if critical conditions take place this certainly happens in point 2 (the case is different if there is a safety valve instead of a rupture disk), so we have $\eta_2 = \eta_c$ and, for (A.3):

$$G_c^* = \frac{\eta_2}{\sqrt{\omega}} \quad (\text{A. 6})$$

If we know ω , N_t and Fi , then (A.1), (A.2) and (A.6) make up virtually a solvable system of three equations with three unknowns ($G^* = G_1^* = G_c^*, \eta_1, \eta_2$).

But in practice N_t is not exactly known a priori, because the cross section of disk and pipe is not known; therefore the calculation procedure is necessarily by trial and error.

Before coming to define the calculation method for G (more straightforward and simple) outlined in par. 1.3.2, we make a mention of the rigorous (but troublesome) procedure which allows to face also the cases of flow in subcritical conditions:

- 1) A trial value is assumed for the pipe cross section (A); so, from (1.16), which gives in practice the value of $G \cdot A$, G (and then $G^* = G/\sqrt{P_0/v_0}$) is calculated.
- 2) N_t is evaluated (as the sum of the contributions of the various pressure losses).
- 3) From (A.1) η_1 is calculated, setting $G_1^* = G^*$.
- 4) From (A.3) η_c is calculated, setting $G_c^* = G^*$. At this point two cases may occur:
 - 5.1) If it is $\eta_c > P_a/P_0$ (where P_a is the pressure in the discharge environment) then we actually have a flow in critical conditions and therefore $\eta_2 = \eta_c$.
From (A.2) we proceed to the calculation of N_t and compare it with the value obtained at point 2). If the results are different we choose another value for A and repeat the calculation starting from point 1) up to convergence.
 - 5.2) If it is $\eta_c < P_a/P_0$ then the flow is not in critical conditions and therefore $\eta_2 = P_a/P_0$.
From (A.2) we proceed to the calculation of N_t , compare it with the value of point 2) and repeat as above the procedure up to convergence.

The method suggested in par. 1.3.2 is all the same by trial and error (as a pipe diameter must be assumed for N_t calculation), but convergence is quick and there are no transcendental equations and integrals to be solved numerically.

It rests on the hypothesis of critical flow (as it normally happens) and on the introduction of a flow reduction coefficient $C_c = G_c^*/G_{oc}^* = \eta_c/\eta_{oc}$ (as it comes out dividing A.3 by A.4).

In practice the actual critical flow G_c^* is evaluated applying a reduction coefficient C_c to the critical flow G_{oc}^* that would hold if the relief device were simply made up by an ideal nozzle. To prepare the curves [14] or the annexed table T1, which give C_c as a function of N_t , ω and Fi , it is convenient to proceed as follows.

- 1) We fix C_c , ω and Fi
- 2) We get η_{oc} from (A.5)
- 3) We obtain $\eta_2 = \eta_c = C_c \cdot \eta_{oc}$ and $G_c^* = \eta_2/\sqrt{\omega}$
- 4) We get η_1 from (A.1) using the previous value of G_c^* (take into account that the actual flow through the ideal nozzle upstream the pipe is subcritical, if we consider the nozzle as an element cut off from the pipe)
- 5) We obtain N_t from (A.2).

Actually we make so a table of N_t as a function of C_c , ω and Fi , but, once made, it is possible to use it to get (through interpolation) C_c as a function of N_t , ω and Fi . On the other hand the implicit form of the available equations does not allow a direct procedure.

Table T1, made as above shown, extends even beyond the range of the values of ω , Fi and N_t of practical use.

For the reactors in the normal regime of two-phase discharge ω varies in fact between 10 and 40, Fi does not exceed 0.1 (except in case of unusual and unsuitable elevations) and N_t stands between 0.5 and 10 (except in case of very long and tortuous pipes).

For $Fi = 0$ (as it happens in case of all vapour flow) we reported also the values of C_c for $\omega = 0.9$, $\omega = 1$, $\omega = 1.2$ and $\omega = 1.5$ (which actually belong to the range of ω values typical of gaseous flow).

Restricting further the analysis to the ranges of values of greater practical interest, it was possible to find some explicit approximate expressions for C_c , very useful to speed up the complex calculations of the rigorous method and for computerized applications.

For $10 \leq \omega \leq 40$, $0 \leq Fi \leq 0.05$ and $C_c \geq 0.6$ (to be checked a posteriori), the following formulas give C_c with an average error of 0.15% and a maximum error of 0.6%:

$$C_c = \frac{1}{1 + a \cdot N_t^b} \quad (\text{A. 7})$$

with:

$$a = 0.2169 - 4.18 \cdot 10^{-3} \omega + 9.55 \cdot 10^{-5} \omega^2 - 8.67 \cdot 10^{-7} \omega^3 + 1.21 \cdot Fi$$

$$b = 0.771 - 0.077 \cdot \exp(-22 \cdot Fi^{0.74})$$

For $Fi = 0$, $0.85 \leq \omega \leq 1.5$ and $C_c \geq 0.3$ the following formulas give C_c with an average error of 0.1% and a maximum error of 0.4%:

$$C_c = \left(\frac{1}{1 + a \cdot N_t^b} \right)^{0.58} \quad (\text{A. 8})$$

with $a = 0.5426 - 0.0541 \omega$
 $b = 0.8456 - 0.0184 \omega$

Table T1

Flow reduction coefficient C_c in critical regime
(listed figures are corresponding N_t values)

	$C_c \rightarrow$	0.9	0.85	0.8	0.75	0.7	0.65	0.6	0.55	0.5	0.4	0.3
Fi = 0	$\omega = 0.9$	0.3384	0.5967	0.9290	1.354	1.900	2.605	3.524	4.742	6.384	11.89	24.20
	1	0.3426	0.6057	0.9449	1.380	1.938	2.660	3.602	4.851	6.536	12.19	24.81
	1.2	0.3504	0.6223	0.9740	1.426	2.008	2.761	3.746	5.050	6.813	12.72	25.93
	1.5	0.3608	0.6443	1.013	1.488	2.101	2.895	3.935	5.314	7.177	13.43	27.39
	10	0.5007	0.9382	1.524	2.292	3.292	4.595	6.301	8.564	11.62	21.82	
	20	0.5845	1.110	1.816	2.742	3.944	5.507	7.549	10.25	13.89	26.01	
	30	0.6443	1.231	2.018	3.048	4.384	6.117	8.378	11.37	15.38	28.74	
	40	0.6921	1.326	2.176	3.286	4.723	6.583	9.009	12.21	16.51	30.79	
Fi = 0.01	$\omega = 10$	0.4660	0.8626	1.384	2.053	2.903	3.979	5.344	7.086	9.331	16.17	
	20	0.5321	0.9952	1.602	2.378	3.357	4.588	6.139	8.107	10.63	18.31	
	30	0.5773	1.083	1.745	2.585	3.641	4.964	6.627	8.731	11.43	19.63	
	40	0.6121	1.150	1.851	2.738	3.849	5.238	6.981	9.184	12.01	20.60	
Fi = 0.02	$\omega = 10$	0.4363	0.8003	1.272	1.871	2.620	3.556	4.725	6.193	8.055	13.58	
	20	0.4899	0.9073	1.448	2.130	2.981	4.040	5.358	7.013	9.113	15.38	
	30	0.5257	0.9772	1.561	2.295	3.209	4.343	5.757	7.531	9.787	16.55	
	40	0.5530	1.030	1.644	2.417	3.377	4.568	6.053	7.917	10.29	17.43	
Fi = 0.03	$\omega = 10$	0.4105	0.7477	1.181	1.725	2.402	3.239	4.276	5.568	7.193	11.95	
	20	0.4549	0.8371	1.329	1.945	2.710	3.656	4.829	6.294	8.143	13.62	
	30	0.4843	0.8954	1.424	2.087	2.908	3.925	5.188	6.767	8.767	14.72	
	40	0.5067	0.9396	1.496	2.193	3.058	4.129	5.459	7.127	9.242	15.57	
Fi = 0.05	$\omega = 10$	0.3679	0.6633	1.039	1.505	2.080	2.784	3.650	4.719	6.051	9.895	
	20	0.3998	0.7302	1.152	1.680	2.331	3.133	4.123	5.354	6.900	11.43	
	30	0.4212	0.7750	1.229	1.797	2.500	3.369	4.444	5.786	7.478	12.48	
	40	0.4378	0.8099	1.288	1.888	2.632	3.552	4.694	6.121	7.926	13.29	
Fi = 0.1	$\omega = 10$	0.2938	0.5227	0.8103	1.165	1.598	2.125	2.767	3.555	4.529	7.298	
	20	0.3106	0.5642	0.8884	1.293	1.793	2.408	3.166	4.104	5.276	8.677	
	30	0.3231	0.5951	0.9463	1.388	1.936	2.613	3.451	4.493	5.803	9.639	
	40	0.3337	0.6209	0.9939	1.465	2.051	2.777	3.677	4.801	6.218	10.39	

To get η_c and G_c , the values of C_c obtained from table T1 or through formulas (A.7) and (A.8) must be coupled (as multipliers) to the values of η_{oc} and G_{oc} given by (1.29) and (1.30). Actually (1.30) is identical to (A.4) and (1.29) practically coincides with (A.5).

Also the value of flow G^* in subcritical conditions, directly obtainable with the complex method previously outlined, can be expressed through suitable reduction coefficients to be applied to the critical flows G_{oc}^* and G_c^* above defined.

We have

$$G^* = C_D \cdot G_{oc}^* = C_F \cdot G_c^* \quad \text{with} \quad C_D = C_F \cdot C_c$$

For $Fi = 0$ and ω equal about to 1 it is possible, with a good approximation, to correlate C_F with the sole parameter $(\eta - \eta_c)/(1 - \eta_c)$, where $\eta = P_a/P_0$ and $\eta_c = C_c \eta_{oc}$.

The simple relation is

$$C_F^2 + \left(\frac{\eta - \eta_c}{1 - \eta_c} \right)^2 = 1 \quad (\text{A.9})$$

which comes from the empirical elliptic law of flow rates (utilized for instance in the field of turbine engines).

The variation of the gaseous flow with the increase of backpressure P_a (for the same P_0) is represented by a curve (fig. 12) very similar to a quarter of ellipse, whose equation is well-known:

$$\left(\frac{G^*}{G_c^*} \right)^2 + \left(\frac{P_a - P_c}{P_0 - P_c} \right)^2 = 1$$

from which (A.9) follows.

Besides notice that, for P_a values not too bigger than P_c , the flow is still practically equal to the critical one. In figures: if $\frac{\eta - \eta_c}{1 - \eta_c} < 0.2$, we have essentially $C_F = 1$.

(A.9) is only approximate, because actually the exponents of C_F and $\frac{\eta - \eta_c}{1 - \eta_c}$ are not exactly equal to 2, but depend on N_t (the error on C_F is however of about 1÷2%; it may reach 5÷6% only for η very close to 1).

If ω is appreciably different from 1 and Fi is different from 0, then (A.9) is no longer valid (in practice the exponents turn out to be a function not only of N_t , but, even more heavily, of ω and Fi). It is then necessary to resort to the complex method, with the numerical solution of (A.1) and (A.2) and the unavoidable trial and error procedure.

Luckily, rare are the cases in which, with $\omega \gg 1$, it is necessary to evaluate C_F , because in two-phase flow conditions it is sufficient to have downstream pressures not much lower than the upstream one to go into the critical regime.

In literature [10;14] a chart is found, valid only for $Fi = 0$, which gives C_F as a function of $(1 - \eta)/(1 - \eta_c)$, for various ω values. From the curve corresponding to $\omega = 1$ it is possible to get C_F values equal to the ones given by (A.9). The curves corresponding to ω values progressively growing (up to $\omega = 40$) are actually largely approximate (with errors higher than 10%), owing to the fact that the correlation between C_F and $(1 - \eta)/(1 - \eta_c)$ does not completely remove the dependence of C_F on N_t (and the higher is ω , the truer this statement).

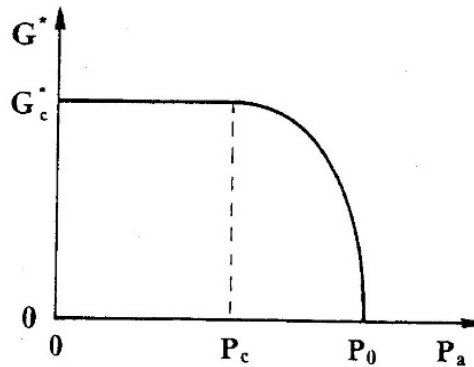


Fig. 12 – Plot of flow rate versus backpressure

APPENDIX II

SAFETY VALVE SIZING

A. II. 1 Valve and pipe sizing

In case a safety valve, instead of a rupture disk, should be chosen as the emergency relief device, the following differences in the calculation method must be taken into account [14;20]:

- 1) A safety valve can be considered fully open when the differential pressure between inlet and outlet becomes 10% higher than the valve set pressure (P_{set}).

In practice, if P_a is the pressure in the discharge environment, flow is conservatively assumed to start at a pressure $P_s = P_a + 1.1 \cdot P_{set}$.

Referring to the example of chapter 4, a pressure $P_s = 1.7$ bara for starting flow with a pressure $P_a = 1.08$ bara in the discharge environment entails a valve set at a differential pressure $P_{set} = (1.7 - 1.08) / 1.1 = 0.564$ bar.

- 2) The valve nozzle (or orifice) is assumed to be the flow controlling element.

It may be approximately assimilable to an ideal frictionless nozzle.

Actually a typical value for the coefficient of discharge of a safety valve, to be applied to the flow through an ideal nozzle, is 0.975.

A further correction factor equal to 0.9 is provided by ASME for certified valves.

To conclude, the nozzle flow area is obtained from (1.16) using for G the value \overline{G}_{oc} given by (1.31) and multiplied by a suitable reduction factor (equal to $0.8775 = 0.975 \cdot 0.9$ if the afore-mentioned coefficients are used).

- 3) In order to avoid unstable valve operation and to assure that its orifice is actually the flow controlling element, inlet and outlet piping must be sized so as:

- the (nonrecoverable) pressure loss ΔP_i upstream the valve does not exceed 3% of P_{set}
- the pressure difference ($P_1 - P_a$) between the nozzle outlet and the discharge environment does not exceed 10% of P_{set} (this limit can however rise up to 50% in the case of balanced-type valves, depending on the models).

For the purpose of these two checks the fluid in the reactor must be considered at pressure P_s ; besides the flow to be taken into account is the actual one according to some authors (that we will follow) and the certified one according to others.

Coming to a practical example, let us suppose to have a valve with measured and certified coefficients respectively equal to 0.98 (C_{ve}) and to $0.98 \cdot 0.9 = 0.882$ (C_{vc}).

The calculations already made in chapter 4 led (supposing $\Delta H = 11$ kcal/mole) to a vent rate W equal to

$$W = \bar{G} \cdot A = \frac{M}{t_e} = \frac{15,000}{98.5} = 152.3 \text{ kg/sec}$$

We got then $\bar{G}_{oc} = \bar{G}/C_c = 1540/0.716 = 2151 \text{ kg/sec/m}^2$.

Both W and \bar{G}_{oc} remain unchanged whichever is the relief device (being identical the physical-chemical and geometric parameters relevant to the reactor).

The relief area, that is the nozzle cross section, is therefore

$$A = W/(\bar{G}_{oc} \cdot C_{vc}) = 152.3/(2151 \cdot 0.882) = 0,0803 \text{ m}^2$$

which corresponds to a nozzle diameter D_n of 319.7 mm.

Actually a valve is available with $D_n = 320$ mm and a cross section $A_n = 0,0804 \text{ m}^2$ (usually it is necessary to choose the valve which has a nozzle area immediately larger than the calculated value). Inlet and outlet flanges have besides diameters D_i and D_v respectively equal to 400 and 500 mm.

For checking point 3) we must calculate the rate W_s vented in the starting discharge conditions, when reactor pressure is P_s (in the following instants overpressure rises much more than backpressure, and therefore the valve operating conditions become less critical).

For this purpose we evaluate the ω parameter with (1.25) for $P = P_s$ (when $v = V/M$):

$$\omega_s = \left(1 - \frac{15,000}{18 \cdot 1100}\right) \cdot \left(1 - 2 \cdot \frac{1.7 \cdot 10^5}{2.157 \cdot 10^6}\right) + \frac{15,000}{18} \cdot \frac{2930 \cdot 388.2 \cdot 1.7 \cdot 10^5}{(2.157 \cdot 10^6)^2} = 0.20 + 34.6 = 34.8$$

where we used the value $\lambda/(v_g - v_l) = 2.157 \cdot 10^6$ already calculated in par. 4.4 for $P = P_s$.

From (1.29) we get $\eta_{oc,s} = 0.922$ and from (1.30)

$$G_{oc,s} = 0.922 \sqrt{\frac{1.7 \cdot 10^5 \cdot 15,000}{18 \cdot 34.8}} = 1860 \text{ kg/sec/m}^2.$$

The vent rate, taking into account the actual values of the coefficient of discharge and of the nozzle area of the chosen valve, is worth

$$W_s = G_{oc,s} \cdot C_{ve} \cdot A_n = 1860 \cdot 0.98 \cdot 0.0804 = 146.6 \text{ kg/sec}.$$

The term ΔP_i of the first check of point 3) is worth

$$\Delta P_i = \frac{v_i}{2} \left(\frac{W_s}{A_i} \right)^2 \cdot N_i$$

where the subscript i refers to the inlet piping (in which the specific volume of the two-phase mixture is v_i), the cross section is A_i and the number of velocity heads corresponding to pressure losses is N_i .

As a rule it is always convenient that the safety valve is close to the reactor. Even more so in our case, in which P_{set} (and therefore ΔP_i) are very low.

If L_{ei} is the equivalent length of the inlet piping, we have $N_i = 0.5 + L_{ei} / D_i / 50$, where 0.5 is due to the square cut pipe entrance and 50, as we saw in par. 1.3.2, is the number of diameters which causes a pressure loss equivalent to one velocity head.

For v_i Leung [20] suggests to adopt, as a first approximation, the value corresponding to a pressure equal to 98% of P_s . From (1.24) we have

$$v_i = \frac{V}{M} \left[\omega_s \left(\frac{P_s}{P_s \cdot 0.98} - 1 \right) + 1 \right] = \frac{18}{15,000} \left[34.8 \left(\frac{1}{0.98} - 1 \right) + 1 \right] = 2.05 \cdot 10^{-3} \text{ m}^3/\text{kg}$$

Assuming for D_i a value of 0.4 m (equal to the diameter of the valve inlet flange) and equating ΔP_i to $0.03 \cdot P_{set} = 1692 \text{ N/m}^2$, we get a maximum value for N_i equal to 1.21 (0.71 excluding the entrance loss) and a maximum equivalent length of piping equal to 14.2 m.

The calculation for checking the outlet piping condition is quite more difficult, because it entails the solution of the integral (A.2) of Appendix I.

More exactly we first calculate the flow G in the tail pipe, supposed at first with a cross section A_p equal to the one of the valve outlet flange (A_v).

We have $G = W_s / A_p = 146.6 / 0.1963 = 747 \text{ kg/sec/m}^2$ and therefore

$$G^* = G / \sqrt{P_0 / v_0} = G / \sqrt{P_s \cdot M / V} = 747 / \sqrt{1.7 \cdot 10^5 \cdot 15,000 / 18} = 0.0628.$$

This flow corresponds to a critical pressure P_p , at the end of the pipe with cross section $A_p = A_v$, given by, owing to (A.3):

$$P_p / P_s = \eta_p = G^* \sqrt{\omega_s} = 0.0628 \sqrt{34.8} = 0.370.$$

As it comes out $\eta_p = 0.370 < P_a / P_s = 1.08 / 1.7 = 0.635$, the flow in the duct is not in critical regime and therefore the pressure P_2 at the end of the same duct is worth P_a ($P_2 / P_s = \eta_2 = P_a / P_s = 0.635$).

As for the outlet piping we know its length (24 m) and the presence of 3 long-radius 90° elbows. With a 0.5 m diameter we have therefore $N_t = 24 / 0.5 / 50 + 3 \cdot 0.25 = 1.71$.

The discharge point is about 1.5 m higher than the valve outlet flange. Therefore:

$$Fi = \frac{Hg}{N_t P_s V/M} = \frac{1.5 \cdot 9.81}{1.71 \cdot 1.7 \cdot 10^5 \cdot 18/15,000} = 0.0422$$

We have now all the elements to solve numerically the integral (A.2) by trial and error, getting η_1 (the upper limit of the integration interval) which is the only unknown.

We get $\eta_1 = 0.724$ and then $P_1 = 0.724 \cdot 1.7 = 1.231$ bara (which is the pressure downstream the nozzle). Then $P_1 - P_a = 1.231 - 1.08 = 0.151$ bar, which represents 27% of P_{set} (this is a percentage that a balanced valve can easily bear).

If we would like to respect the limit of 10% (to use a conventional unbalanced valve), then P_1 should be equal to $1.08 + 0.1 \cdot 0.564 = 1.136$ bara and therefore $\eta_1 = P_1/P_s = 0.668$.

It is then necessary to increase A_p (which affects the value of G^* , of N_t and of Fi) so that (A.2) is respected with that value of η_1 . In our case we obtain a pipe diameter of 620 mm.

The artifice of increasing the diameter to decrease the backpressure is valid till the valve exit becomes the element determining critical flow conditions, after which it is obvious that it is no use enlarging the pipe, because the pressure in the valve body remains at the aforesaid critical value.

In our case this is not a problem, because we checked that, for a 500 mm diameter (equal to the one of the valve outlet flange), η_p turns out to be 0.370, which is lower than $P_a/P_s = 0.635$.

But with higher pressures P_s (of the order of 4÷5 bara) the problem may occur, and then the only solution to avoid instability and lack of vent capacity is to choose, if possible, a valve with a greater A_v/A_n or of balanced type.

We will try to better explain this problem with an example.

For mass conservation we have $G_n \cdot A_n = G_v \cdot A_v = G_p \cdot A_p$ (where the subscripts n , v and p refer respectively to nozzle, valve exit and tail pipe). Besides $G_n = C_{ve} \cdot G_{oc}$ and (in critical conditions)

$$\eta_n/G_n = \eta_{oc}/G_{oc} = \eta_v/G_v = \eta_p/G_p = \sqrt{\omega_s}/\sqrt{P_s \cdot M/V}$$

From the previous relations we get

$$\eta_v = \eta_{oc} \cdot C_{ve} \cdot A_n/A_v \quad \text{and} \quad \eta_p = \eta_{oc} \cdot C_{ve} \cdot A_n/A_p$$

As (in the range of ω values typical of two-phase flow) $\eta_{oc} \sim 0.9$ and (for big valves) $A_v/A_n = 2.5 \div 3$, we have $\eta_v = 0.3 \div 0.35$.

Let us assume then $\eta_v = 0.3$ and let us suppose that $P_s = 4.5$ bara and $P_a = 1$ bara, so that $P_{set} = (4.5 - 1) / 1.1 = 3.18$ bar and $P_v = 4.5 \cdot 0.3 = 1.35$ bara (which is the critical pressure corresponding to the cross section A_v).

If the tail pipe has an area $A_p = A_v$, then at its exit we have a critical pressure P_p equal to P_v , because $\eta_p = \eta_v = 0.3 > P_a/P_s = 0.222$.

The pressure P_1 immediately downstream the nozzle will be certainly greater than P_v and can be obtained by trial and error (in the form of η_1) through the usual integral, setting $\eta_2 = \eta_v$ and $G^* = \eta_v \sqrt{\omega_s}$.

As $(P_1 - P_a) > (P_v - P_a) = 0.35$ bar, it will be certainly impossible to satisfy the condition $(P_1 - P_a) < 0.1 \cdot P_{set} = 0.318$ bar.

If we progressively increase A_p over A_v , the exit pressure P_p will decrease in inverse proportion ($P_p = P_v \cdot A_v/A_p$), always remaining critical until greater than P_a .

In this way P_1 will decrease down to the value of P_v , but it will never become lower, because in that moment the valve exit is going to be critical. Accordingly $P_1 - P_a$ will never become lower than 0.35 bar, and therefore it will not certainly be able to respect the limit of 10% of P_{set} (0.318 bar).

If on the contrary $P_s = 4$ bara, then $P_{set} = 2.73$ bar and $P_v = 1.2$ bara. With $A_p = A_v$ we would have $(P_1 - P_a) > (P_v - P_a) = 0.2$ bar and probably it would be impossible to satisfy the condition $(P_1 - P_a) < 0.1 \cdot P_{set} = 0.273$ bar. But increasing suitably A_p it will be certainly possible to lower P_1 down to P_v (1.2 bara) and therefore $P_1 - P_a$ down to 0.2 bar, so respecting the aforesaid condition.

In the case of gas or vapour vent the same remarks hold (besides the constancy of the ratio η/G in critical conditions, whichever section is considered, is a result obtainable not only with the “ ω ” method, but also with the classic theory that leads to the Lapple-Levenspiel diagrams).

The only difference is that η_{oc} is worth about 0.6 and therefore $\eta_v = 0.2 \div 0.24$.

It follows that the problems of potential instability occur for much higher P_s values (about twice as much as in the two-phase flow conditions).

A. II. 2 Thrust calculation

Another remarkable difference in comparison with the rupture disk calculation may be found in the evaluation of the thrust on piping.

(1.36) and (1.37) still hold, taking into account that they refer however to the pipe exit conditions and that therefore G is the specific flow in the tail pipe (G_p), and not in the nozzle (G_n).

While in the disk case the discharge from the outlet pipe normally takes place in the critical regime, in the valve case the flow through the nozzle is critical, but the conditions at the tail pipe exit may anyway come out to be subcritical (as we just saw in the example of the previous paragraph).

If the tail pipe exit conditions are critical, then in that point we have $\eta_p = \eta_{oc} \cdot C_{ve} \cdot A_n/A_p$, as we obtained above.

In this case not only the expression (1.37) is still valid, but also (1.38), where it is sufficient to replace η_c with the value of η_p calculated as above. Therefore if $\eta_p > P_a/P_0$:

$$\bar{T} = \frac{T}{P_0 A_p} + \frac{P_a}{P_0} = \left(\frac{1}{\omega} - 1 \right) \eta_p^2 + 2\eta_p \quad (\text{A. 10})$$

If on the contrary $\eta_p < P_a/P_0$, then (1.36) holds. Taking into account (1.24) and the fact that

$$\frac{G_p^2 v_0}{P_0} = \frac{G_n^2 v_0}{P_0} \left(\frac{A_n}{A_p} \right)^2 = \frac{G_{oc}^2 v_0}{P_0} \cdot C_{ve}^2 \left(\frac{A_n}{A_p} \right)^2 = \frac{\eta_{oc}^2}{\omega} \cdot C_{ve}^2 \left(\frac{A_n}{A_p} \right)^2 = \frac{\eta_p^2}{\omega}$$

we have:

$$\frac{T}{P_0 A_p} = \frac{v_a}{v_0} \frac{G_p^2 v_0}{P_0} = \eta_p^2 \left(\frac{1}{\omega} + \frac{P_0}{P_a} - 1 \right) \quad (\text{A. 11})$$

It is interesting to notice that, once A_p has been fixed, the thrust value (both in critical and in subcritical conditions) does not depend on the tail pipe length and course, as it happened instead in the disk case. Only the conservative choice of disregarding the presence of the pipe downstream the disk made the thrust value practically independent of the pipe course.

Also in the case of safety valve relief there are transient phenomena which may lead to instantaneous thrust values higher than the steady-state ones. Such phenomena are however much more moderate than in the disk case.

It is usual however to disregard the downstream piping also in this case, which has besides less remarkable effects on the result.

Actually it is a question of replacing A_p with A_v in the previous formulas. In the frequent case in which the tail pipe has the same diameter as the valve outlet flange, the thrust value remains for instance the same.

Now too we assume conservatively for P_0 the maximum value of the pressure in the reactor (P_m) and we multiply by 2 the final result to take into account the dynamic effects.

If the emission were made up by pure vapour, the thrust value (with the same P_0) might be higher than in the two-phase regime just in the case of subcritical exit flow and low P_0 values.

In fact in the critical regime, when (A.10) holds, we can easily check that the \bar{T} values for ω equal to about 1 are always lower than the ones obtained for $\omega = 10 \div 40$.

On the contrary in subcritical conditions, when (A.11) holds, for P_0/P_a lower than about 1.8 we get higher T values in the case of vapour vent ($\omega = \sim 1$).

But, once A_n has been fixed, the maximum pressure in the reactor is certainly higher in conditions of two-phase discharge (in our example we have $P_0 = P_m = 2.6$ bara, against a value of 1.7 bara, equal to P_s , which would certainly correspond to the maximum pressure in case of all vapour emission).

Therefore the T value calculated supposing two-phase conditions is normally more conservative.

In the worked example, taking into account that $\bar{\omega} = 18.7$, $\bar{\eta}_{oc} = 0.890$, $C_{ve} = 0.98$, $A_n/A_v = 0.41$, $A_v = 0.1963$ m² and assuming conservatively $P_0 = 2.6$ bara, $P_a = 1$ bara and $A_p = A_v$, we get:

$$\eta_p = \bar{\eta}_{oc} \cdot C_{ve} \cdot \frac{A_n}{A_v} = 0.890 \cdot 0.98 \cdot 0.41 = 0.358 < \frac{P_a}{P_s} = \frac{1}{1.7} = 0.588 \text{ (subcritical regime)}$$

and then from (A.11), applying the safety factor 2:

$$T = 2 \cdot 2.6 \cdot 10^5 \cdot 0.1963 \cdot 0.358^2 (1/18.7 + 2.6/1 - 1) = 21,600 \text{ N} = 2200 \text{ kg}$$

For $\omega = 0.88$ (pure vapour, as calculated in par. 4.4) we have

$$\eta_{oc} = 0.59 \text{ and } \eta_p = 0.59 \cdot 0.98 \cdot 0.41 = 0.237.$$

At last from (A.11), with $P_0 = P_s = 1.7$ bara, we get

$$T = 2 \cdot 1.7 \cdot 10^5 \cdot 0.1963 \cdot 0.237^2 (1/0.88 + 1.7/1 - 1) = 6900 \text{ N} = 700 \text{ kg}$$

which confirms that the most conservative value is the one referring to the two-phase regime.

APPENDIX III

MEAN VALUE OF SPECIFIC THERMAL POWER

The mean value of specific thermal power q (W/kg) in the range between T_s and T_m , to be inserted in the Leung formula, is traditionally calculated considering the arithmetic mean M_a of the two values, $\left(\frac{dT}{dt}\right)_{ps}$ and $\left(\frac{dT}{dt}\right)_{pm}$, assumed by $\left(\frac{dT}{dt}\right)_p$ at the two ends of the range.

To face some problems emerging in case of remarkable differences between T_s and T_m (that is in case of high overpressures), also the geometric mean M_g and the logarithmic mean M_l have been considered.

Actually, if we want to take into account the remarkable variation of $\left(\frac{dT}{dt}\right)_p$ during venting, especially in case of high overpressures, it is necessary to consider also the extension in time of the effect of a certain level of thermal power.

Practically, if we have at our disposal the plot of temperature versus time (during venting), and therefore the plot of $\left(\frac{dT}{dt}\right)_p$ (which is a function of temperature) versus time, it is possible to calculate the following integral mean:

$$M_i = \frac{\int_0^{t_m} \left(\frac{dT}{dt}\right)_p \cdot dt}{t_m}$$

It represents (excluding the factor $M \cdot C_p$) the total heat generated during the critical phase of venting and referred to its length t_m , that is the effective mean thermal power in the period of interest.

The main problem for M_i calculation is that the value of t_m , available through Leung formulas, depends on q , that is on the mean value chosen for $\left(\frac{dT}{dt}\right)_p$, which seems to involve a tedious trial and error procedure.

Actually the integral mean can be expressed as:

$$M_i = \int_0^1 \left(\frac{dT}{dt}\right)_p \cdot d\left(\frac{t}{t_m}\right)$$

where $\left(\frac{dT}{dt}\right)_p$ can be expressed as a function of t/t_m with a formula which does not depend on q and which allows the calculation of M_i before applying Leung formulas.

As shown below, the diagram of temperature between $t = 0$ and $t = t_m$ (that is $t/t_m = 1$) is given by:

$$T = T_s + \Delta T \cdot \frac{t}{t_m} \cdot \left(1 + b - \frac{b^2}{1 + b - \frac{t}{t_m}}\right) \quad \text{with} \quad b = \sqrt{\frac{V \cdot \bar{T} \cdot \Delta P}{M \cdot C_p \cdot \Delta T}}$$

If we know the kinetic expression that binds $\left(\frac{dT}{dt}\right)_p$ to T , the integral can be directly calculated (by numerical solution).

On the contrary if we dispose of the listed values of $\left(\frac{dT}{dt}\right)_p$ versus T , given by a VSP test, we can calculate, by the previous formula, the T values corresponding for instance to $t/t_m = 0 - 0.125 - 0.25 - 0.375 - 0.5 - 0.625 - 0.75 - 0.875 - 1$. From the VSP list we get the 9 values (a_0, a_1, \dots, a_8) of $\left(\frac{dT}{dt}\right)_p$ corresponding to the 9 calculated temperatures. Using at last the Cavalieri-Simpson formula we get immediately, with good approximation:

$$M_i = [a_0 + 4(a_1 + a_3 + a_5 + a_7) + 2(a_2 + a_4 + a_6) + a_8]/24$$

Usually, M_i is nearer to the arithmetic mean than to the geometric or logarithmic mean.

Besides, the difference between M_i and M_a is very small, even with rather high overpressures.

The diagram of temperature versus time during venting, between $t = 0$ and $t/t_m = 1$, can be obtained through a suitable elaboration of the differential equation that brings to the Leung formula:

$$mq = mC_p \frac{dT}{dt} + GA \frac{V}{m} \cdot \frac{\lambda}{v_g - v_l}$$

Here $\frac{dT}{dt}$ has obviously a quite different meaning than $\left(\frac{dT}{dt}\right)_p$, which is referred to the results of a test in a non-venting apparatus.

As $m = M - GAt$, with $m = 0$ for $t = t_e = \frac{M}{GA}$, we have $m = GA(t_e - t)$.

Besides, for the Clapeyron equation, we will consider $\frac{\lambda}{v_g - v_l} = \bar{T} \cdot \frac{\Delta P}{\Delta T}$.

The differential equation then becomes:

$$q = C_p \frac{dT}{dt} + \frac{t_e}{(t_e - t)^2} \cdot \frac{V \bar{T} \Delta P}{M \Delta T}$$

Setting $\frac{V \bar{T} \Delta P}{M \Delta T} = a$, and naming t_m the t value for which $\frac{dT}{dt} = 0$, we get $q = \frac{t_e}{(t_e - t_m)^2} \cdot a$ and

$$qt_m = \frac{\frac{t_e}{t_m}}{\left(\frac{t_e}{t_m} - 1\right)^2} \cdot a \quad (\text{A.12})$$

Integrating the differential equation, with the condition that $T = T_s$ for $t = 0$, we get:

$$C_p(T - T_s) = t \left(q - \frac{a}{t_e - t} \right) \quad (\text{A.13})$$

Setting $T = T_m$ for $t = t_m$, we get (being $T_m - T_s = \Delta T$ and setting $C_p \cdot \Delta T = c$)

$$c = qt_m - \frac{a}{\frac{t_e}{t_m} - 1} \quad (\text{A.14})$$

From the system of the two equations (A.12) and (A.14) we get:

$$qt_m = c \left(1 + \sqrt{\frac{a}{c}} \right) \quad \frac{t_e}{t_m} = 1 + \sqrt{\frac{a}{c}}$$

From the expression (A.13) then we obtain:

$$T = T_s + \frac{1}{C_p} \frac{t}{t_m} \left(qt_m - \frac{a}{\frac{t_e}{t_m} - \frac{t}{t_m}} \right) = T_s + \frac{\Delta T}{c} \frac{t}{t_m} \left[c \left(1 + \sqrt{\frac{a}{c}} \right) - \frac{a}{1 + \sqrt{\frac{a}{c} - \frac{t}{t_m}}} \right]$$

that is, setting $b = \sqrt{\frac{a}{c}} = \sqrt{\frac{\frac{V \bar{T} \Delta P}{M \Delta T}}{C_p \Delta T}}$,

$$T = T_s + \Delta T \cdot \frac{t}{t_m} \left(1 + b - \frac{b^2}{1 + b - \frac{t}{t_m}} \right)$$

REFERENCES

- [1] Gustin J.L. et al. (1993) - The phenol + formaldehyde runaway reaction. Vent sizing for reactor protection - *J. Loss Prev. Process Ind.*, Vol. 6, No 2, p. 103
- [2] Gustin J.L. (1991) - Calorimetry for emergency relief systems design (in "Safety of Chemical Batch Reactors and Storage Tanks") - Kluwer Academic Publishers
- [3] Leung J.C. et al. (1986) - Thermal runaway reactions in a low thermal inertia apparatus - *Thermochimica Acta*, 104, p. 13
- [4] Martin R.W (1956) - The chemistry of phenolic resins - John Wiley & Sons, Inc.
- [5] Zavitsas A.A. et al. (1968) - *J. Polym. Sci. Part. A-1*, 6, 2541
- [6] Leung J.C. and Epstein M. (1990) - The discharge of two-phase flashing flow from an inclined duct - *Trans. ASME (J. Heat Transfer)*, 112, p. 524
- [7] Jones T.T. (1946) - *J. Soc. Chem. Ind.*, 65, 264
- [8] British Plastics Federation (1979) - Guidelines for the safe production of phenolic resins
- [9] Leung J.C. (1986) - Simplified vent sizing equations for emergency relief requirements in reactors and storage vessels - *AIChE J.*, 32, p. 1622
- [10] Leung J.C. and Fisher H.G. (1989) - Two-phase flow venting from reactor vessels - *J. Loss Prev. Process Ind.*, Vol. 2, April, p. 78
- [11] Leung J.C. (1992) - Venting of runaway reactions with gas generation - *AIChE J.*, 38, p. 723
- [12] Duxbury H.A. and Wilday A.J. (1990) - The design of reactor relief systems - *Process Safety Environ.*, 68B, 24
- [13] Leung J.C. (1986) - A generalized correlation for one-component homogeneous equilibrium flashing choked flow - *AIChE J.*, 32, p. 1743
- [14] Design Institute for Emergency Relief Systems (1992) - Project Manual, AIChE
- [15] Leung J.C. (1987) - Overpressure during emergency relief venting in bubbly and churn-turbulent flow - *AIChE J.*, 33, p. 952
- [16] Leung J.C. and Fauske H.K. (1987) - Runaway system characterization and vent sizing based on DIERS methodology - *Plant/Operations Progress*, 6, p. 77
- [17] Lapple C.E. (1943) - Isothermal and adiabatic flow of compressible fluids - *Trans. AIChE*, 39, p. 385

- [18] Levenspiel O. (1977) - The discharge of gases from a reservoir through a pipe - AIChE J., 23, p. 402
- [19] Huff J.E. and Shaw K.R. (1992) - Measurement of flow resistance of rupture disk devices - Plant/Operations Progress, 11, p. 187
- [20] Leung J.C. (1992) - Size safety relief valves for flashing liquids - Chem. Eng. Progress, 88 (2), p. 70
- [21] Leung J.C. (1995) - The omega method for discharge rate evaluation - International Symposium on runaway reactions and pressure relief design, AIChE/DIERS
- [22] CCPS/AICHE/DIERS (2017) – Guidelines for pressure relief and effluent handling systems (second edition) – John Wiley & Sons, Inc.